

Online Research @ Cardiff

This is an Open Access document downloaded from ORCA, Cardiff University's institutional repository: <https://orca.cardiff.ac.uk/id/eprint/125167/>

This is the author's version of a work that was submitted to / accepted for publication.

Citation for final published version:

Barker, Stephen ORCID: <https://orcid.org/0000-0001-7870-6431>, Knorr, Gregor, Conn, Stephen, Lordsmith, Sian, Newman, Dhobasheni and Thornalley, David 2019. Early interglacial legacy of deglacial climate instability. *Paleoceanography and Paleoclimatology* 34 (8) , pp. 1455-1475. 10.1029/2019PA003661 file

Publishers page: <http://dx.doi.org/10.1029/2019PA003661>
<<http://dx.doi.org/10.1029/2019PA003661>>

Please note:

Changes made as a result of publishing processes such as copy-editing, formatting and page numbers may not be reflected in this version. For the definitive version of this publication, please refer to the published source. You are advised to consult the publisher's version if you wish to cite this paper.

This version is being made available in accordance with publisher policies.

See

<http://orca.cf.ac.uk/policies.html> for usage policies. Copyright and moral rights for publications made available in ORCA are retained by the copyright holders.



Early interglacial legacy of deglacial climate instability

Stephen Barker¹, Gregor Knorr^{1,2}, Stephen Conn¹, Sian Lordsmith¹, Dhobasheni Newman¹ and David Thornalley³

¹ School of Earth and Ocean Sciences, Cardiff University, Cardiff CF10 3AT, UK.

² Alfred Wegener Institute, 27570 Bremerhaven, Germany.

³ Department of Geography, University College London, London, UK

Corresponding author: Stephen Barker (barkers3@cf.ac.uk)

Key Points:

- The relationship between changes in atmospheric CO₂ and surface conditions across the NE Atlantic has been consistent over the past 800kyr
- The ocean/atmosphere system may take thousands of years to re-equilibrate following abrupt deglacial oscillations in ocean circulation
- Inclusion of non-equilibrium intervals within interglacial comparisons may lead to artifacts in calculated trends in e.g. atmospheric CO₂

Abstract

Throughout the last glacial cycle millennial timescale variations in atmospheric CO₂ occurred in parallel with perturbations in deep ocean circulation, which were themselves reflected by observable changes in surface conditions across the North Atlantic region. Here we use continuous proxy records to argue that an equivalent relationship has held throughout the last 800kyr i.e. since before the first occurrence of Heinrich events *sensu stricto*. Our results highlight the importance of internal climate dynamics in amplifying external (insolation) forcing on the climate system to produce the large amplitude of glacial terminations (deglaciations) during the mid to late Pleistocene. We show that terminations are characterized by an interval of intense ice rafting followed by a subsequent and abrupt shift to anomalously warm surface conditions (with respect to the more gradually evolving background state), which we interpret to reflect an abrupt recovery of deep ocean circulation in the Atlantic. According to our synthesis, this is followed by a period of enhanced (or at least anomalous) overturning lasting thousands of years until equilibrium interglacial conditions are attained and during which atmospheric CO₂ is likely to decrease. Our results therefore suggest that deglacial oscillations in ocean circulation can have a lasting influence on early interglacial climate and highlight the transient nature of atmospheric CO₂ overshoots associated with the onset of some previous interglacials. Accordingly we suggest that these intervals should be considered as a part of the deglacial process. This has implications for studies concerned with the evolution of atmospheric CO₂ during interglacial periods including the Holocene.

1 Introduction

This work is dedicated to the memory of Wallace S. Broecker, a friend and mentor, whose impact on paleoceanography and the study of paleoclimate was profound. It is humbling to consider how often we seem to repaint the wheels invented by past leaders in our respective fields. Wally's tracks appear most often within texts on glacial-interglacial CO₂ variability, abrupt climate change and ocean circulation and it seems appropriate then that his 1989 study with George Denton provided such clear foresight to the conclusions of this study.

Reconstructions of ocean circulation and the record of atmospheric CO₂ across Marine Isotope Stage (MIS) 3 and the last deglaciation (Termination, T1) reveal a close coupling between ocean state and CO₂ (Figs. 1-3) with CO₂ rising (on a millennial timescale) while Atlantic Ocean circulation (specifically the Atlantic Meridional Overturning Circulation, AMOC) is in a pronounced weak or shallow mode (particularly those intervals associated with so-called Heinrich events – massive North Atlantic ice rafting events sourced from Hudson Strait [Hemming, 2004]) and decreasing again after recovery to a strong mode, at least during MIS 3 [Ahn and Brook, 2008; Roberts *et al.*, 2010; Marcott *et al.*, 2014; Henry *et al.*, 2016]. An additional century scale rise in CO₂ may also occur as the AMOC recovers [Marcott *et al.*, 2014; Chen *et al.*, 2015; Deaney *et al.*, 2017]. Modelling studies suggest that such changes in CO₂ could be driven by biophysicochemical changes directly associated with variations in deep ocean circulation [Marchal *et al.*, 1998; Kohler *et al.*, 2005; Schmittner and Galbraith, 2008; Sigman *et al.*, 2010; Menviel *et al.*, 2014; Ganopolski and Brovkin, 2017] or indirectly through affiliated changes in atmospheric circulation [Menviel *et al.*, 2008]. For the purposes of this study however, it is the temporal association between changes in ocean circulation and atmospheric CO₂ (implying a mechanistic link) that is of critical interest; we wish to determine whether or not

this association has been consistent over the last 800kyr, during which we have continuous records of atmospheric composition and encompassing a period before the appearance of Heinrich events *sensu stricto* (i.e. derived from Hudson Strait) around 640ka [Hodell *et al.*, 2008; Naafs *et al.*, 2011].

An initial test of this proposition is given by a comparison between changing atmospheric CO₂ and a reconstruction of northern abrupt climate variability, GL_{T_syn_hi} [Barker *et al.*, 2011], which we argue provides a zeroth-order approximation for AMOC strength (see Methods Section 2.3; Fig. 4). The comparison suggests that a major proportion of CO₂ change (in either direction) occurs when the AMOC is furthest from equilibrium. In particular, CO₂ tends to increase while the AMOC is (inferred to be) anomalously weak and decrease when the AMOC is (inferred to be) anomalously strong. Ahn and Brook [2014] demonstrated that atmospheric CO₂ does not necessarily change during shorter stadial events and our analysis does not contradict this. Figure 4 suggests that >50% of the cumulative rise in CO₂ over the last 800kyr coincided with strongly negative values of GL_{T_syn_hi} (which should coincide with stadial conditions across the North Atlantic) but we also note that many instances of negative GL_{T_syn_hi} coincide with unchanging or even decreasing CO₂.



Within this study we use the term ‘equilibrium’ (and ‘quasi-equilibrium’) to reflect a (hypothetical) situation where the climate system (including all its components e.g. mean temperature, ocean circulation, atmospheric CO₂ concentration) is equilibrated (or close to being equilibrated) with respect to Earth’s orbital configuration. Since Earth’s orbit varies continuously we would not expect equilibrium conditions to remain constant but instead to vary on timescales >10³ years. Furthermore, thanks to the inherent non-linearity of Earth’s climatic response to changes in insolation (see below), it is difficult to assess whether any observed climate ‘state’ (e.g. glacial or interglacial) represents anything like a truly equilibrated state. We therefore use the term with caution but nevertheless we think it is useful in the context of millennial-scale variability. We also define ‘anomaly’ as the difference (departure) from more gradually evolving background conditions, in this case a 7kyr smooth of the record under consideration (see Methods Section 2.2.1). In this context, background conditions can be considered as broadly synonymous with equilibrium conditions, with the important caveat noted above that changes in the background state necessarily include non-linear responses to changes in insolation.

Milankovitch [1941] predicted that changes in the integrated intensity of northern hemisphere summer insolation should drive the waxing and waning of continental ice sheets and ultimately the transitions between glacial and interglacial state. However, the forcing due to changing summer insolation alone is not sufficient to explain the large magnitude of deglacial transitions [Imbrie *et al.*, 1993] (known as glacial terminations [Broecker and van Donk, 1970]) and it has long been appreciated that nonlinearities within the climate system are required in order to explain the magnitude of these major climate shifts. Early work suggested that abrupt changes in ocean circulation and their influence on atmospheric CO₂ could play a central role in the mechanism of termination [Broecker and Denton, 1989; Imbrie *et al.*, 1993] and several recent studies have reached an equivalent conclusion based on evidence from various paleoclimate archives [Anderson *et al.*, 2009; Barker *et al.*, 2009; Cheng *et al.*, 2009; Denton *et al.*, 2010; Skinner *et al.*, 2010; Barker *et al.*, 2011; Cheng *et al.*, 2016]. Specifically, a shift in ocean circulation patterns during termination is thought to lead to an increase in CO₂ that can eventually promote the transition to an interglacial state. Here we wish to investigate this link for all of the deglacial transitions of the last 800kyr. In particular, we are interested in the similarities

and differences among individual terminations, and whether these impact the climatic evolution of subsequent interglacial periods.

The gradual rise in atmospheric CO₂ throughout the last 8,000 years of the Holocene (prior to industrialisation) has attracted many possible explanations, ranging from natural (e.g. through changes in the terrestrial biosphere or marine inorganic chemistry [Indermuhle *et al.*, 1999; Broecker *et al.*, 2001; Ridgwell *et al.*, 2003; Elsig *et al.*, 2009; Kleinen *et al.*, 2010]) to anthropogenic influences such as deforestation [Ruddiman, 2003; Ruddiman *et al.*, 2016]. Ruddiman *et al.* [2016] use various comparisons between the Holocene (MIS 1) and earlier interglacials to argue that the Holocene (upward) trend in CO₂ is anomalous and therefore unnatural or anthropogenic. However, according to their analysis only three interglacials (MIS 7, 9 and 19) consistently reveal a decreasing trend (with the additional possibility of MIS 5). Notably these interglacials are themselves unusual because they display so-called overshoots in CO₂ at their onset [Tzedakis *et al.*, 2009] (Fig. 5). If these overshoots actually reflect the transient effects of abrupt deglacial changes in ocean circulation (rather than quasi-equilibrium interglacial conditions) then it could be argued that they should not be included in the definition (and therefore analysis) of interglacial trends in CO₂, in which case the conclusions of Ruddiman *et al.* [2016] may have to be moderated. A recent modelling study by Ganopolski and Brovkin [2017] suggests this might be the case. These authors conclude that the timing of AMOC recovery within a termination is critical for determining the early interglacial level of atmospheric CO₂. For example, if recovery occurs only at the end of termination (e.g. when CO₂ has already reached an interglacial level), a pronounced overshoot in CO₂ will occur, followed by a steady or decreasing trend during the subsequent interglacial (e.g. MIS 5). On the other hand an early AMOC recovery will result in a lower initial CO₂ level, followed by a rise during the subsequent interglacial (e.g. MIS 1). A similar conclusion was reached in a proxy study by Deaney *et al.* [2017], who suggested that the early AMOC recovery associated with the Bølling-Allerød during Termination 1 could explain the smaller apparent magnitude of CO₂ change across T1 as compared with the previous deglaciation (T2) for which AMOC recovery did not occur until the very end of termination, resulting in a transient CO₂ overshoot associated with AMOC recovery during early MIS 5.

To test these ideas more thoroughly requires (ideally) high resolution reconstructions of ocean circulation across multiple terminations as well as during glacial and interglacial periods to assess the connection between ocean circulation and CO₂ change for a variety of timescales and background states. However, unambiguous reconstructions of deep ocean circulation are difficult to obtain and as a result, direct evidence for a temporal link between changes in ocean circulation and atmospheric CO₂ across deglacial transitions is currently limited to the last two terminations (T1 and T2) [Roberts *et al.*, 2010; Deaney *et al.*, 2017]. However, the observed correlation between ocean circulation and surface conditions across the North Atlantic region over the last glacial cycle (weakened circulation is associated with ice rafting and anomalously cold conditions and vice versa; Fig. 2) allows a first order approximation of the relationship between the AMOC and atmospheric CO₂ over this interval to be made using surface conditions as a surrogate for the state of ocean circulation (Methods Section 2.2; Fig. 3). In general CO₂ tends to increase while the North Atlantic region is anomalously cold (reflecting periods of weakened AMOC) and decrease when conditions are anomalously warm (when Atlantic circulation is relatively strong). Note again that we are interested in the temporal relationship between CO₂ and AMOC; this discussion does not address the specific mechanism linking ocean circulation to CO₂ (i.e. it does not imply that a weakening of AMOC directly causes an increase

in CO₂ or vice versa).

In this study we aim to exploit this observation to investigate the relationship between ocean circulation and changing atmospheric CO₂ over the past 800kyr, using proxies for NE Atlantic surface conditions from ODP site 983 (Fig. 1) as a surrogate for the state of ocean circulation within the Atlantic (i.e. strength of the AMOC). Several statistical and modelling studies have suggested a direct link between temperature variations in the subpolar North Atlantic and the strength of AMOC [Zhang, 2008; Dima and Lohmann, 2010; Muir and Fedorov, 2015; Caesar *et al.*, 2018] with observational support for this relationship deriving from the RAPID-AMOC 26°N array [Smeed *et al.*, 2018]. Cooling of the subpolar gyre over the last millennium is thought to be a direct manifestation of weakening AMOC strength [Rahmstorf *et al.*, 2015; Caesar *et al.*, 2018; Thornalley *et al.*, 2018] and this is supported by reconstructions of the Deep Western Boundary Current over the same period [Thornalley *et al.*, 2018]. ODP Site 983 is located within the region of subpolar cooling associated with recent AMOC weakening [Caesar *et al.*, 2018; Smeed *et al.*, 2018] and therefore we suggest that it is in a suitable position for assessing past changes in AMOC strength using this approach. We employ the relative proportion of *Neogloboquadrina pachyderma* (a polar-affiliated species of planktic foraminifera) within the total assemblage (%NPS) to reconstruct fluctuations between polar and subpolar conditions and the millennial-scale component of this (%NPS_{hi}; Methods Section 2.2.1) to identify periods of anomalous cold and warmth. We also use the concentration of lithic grains >150µm (ice rafted debris, IRD) to reflect the transport of icebergs to the open ocean southwest of Iceland. The limitations of our approach are obvious (we are using a single core site to estimate large scale change in AMOC by means of an indirect approach), but we maintain that at the very least our assessment of the link between surface conditions in the NE Atlantic and changes in atmospheric CO₂ will provide a valuable test for climate models and a testing ground for a range of future proxy studies.

2 Materials and Methods

2.1 Sample preparation and age model for ODP site 983

For this study we processed 2,272 samples along the splice of ODP 983 [Jansen *et al.*, 1996]. Each sample was 2cm wide (representing ~170 years on average), taken every 2cm from 0.02 to 1.98 and 51.52 to 94.95 MCD. Previously [Barker *et al.*, 2015] we reported results from the interval 2.0 to 51.5 MCD. Sediment samples were spun overnight and washed with DI water through a 63µm sieve before being dried at 40°C. IRD and faunal counts were made on the >150µm fraction after splitting to yield approximately 300 entities. IRD was considered as the total number of lithogenic/terrigenous grains counted. The majority of grains fall into two categories: quartz and volcanics, with volcanics comprising ~36% of the total IRD on average during the last glacial period [Barker *et al.*, 2015]. Only left coiling specimens of *N. pachyderma* were counted and all 5 morphotypes of *N. pachyderma* found in recent Arctic sediments [Eynaud, 2011] were counted (Fig. S1). We recounted ~1,000 of the samples previously reported [Barker *et al.*, 2015] covering the depth interval 32.04 to 51.5 MCD because of concerns over non-identification of lightly encrusted morphotypes of *N. pachyderma* during the warm stages of MIS 11 (Fig. S2). Our recounts suggest that we had previously underestimated the proportion of *N. pachyderma* during MIS 11 but were correctly calibrated in later warm intervals. We also

checked our taxonomy across MIS 11 by resampling nearby ODP site 980 that was analysed by Oppo et al. [1998]. Our counts are in very good agreement with that study (Fig. S2). We stress that our recounts do not affect the conclusions of our previous study [Barker et al., 2015].

The site of ODP site 983 is positioned on the rapidly accumulating Gardar Drift and sediment accumulation is sensitive to changes in the dense overflows crossing the Iceland-Scotland Ridge [Raymo et al., 2004; Kleiven et al., 2011] which themselves are thought to co-vary with high latitude climate [Kleiven et al., 2011; Ezat et al., 2014]. At orbital timescales this results in elevated sedimentation rates during interglacials (as implied by the LR04 age model [Lisiecki and Raymo, 2005] and noted previously [Barker et al., 2015]) when the overflows are thought to be more vigorous [Raymo et al., 2004; Kleiven et al., 2011]. But this also implies that sedimentation rates are elevated during millennial-scale warm events that are not accounted for by the LR04 age model. It is therefore necessary to tune our records to a target with millennial-scale features and following our previous study [Barker et al., 2015], we use the millennial component of a synthetic reconstruction of northern climate variability (GL_{T_syn_hi}) [Barker et al., 2011] derived from the Antarctic ice core temperature record [Jouzel et al., 2007] on the AICC2012 age model [Bazin et al., 2013] as a tuning target (Fig. S3). Specifically, we align abrupt warming events in our record (which also align with the disappearance of IRD) with warming transitions in GL_{T_syn_hi}. We also align increases in the coarse fraction (>63µm) with cooling transitions in GL_{T_syn_hi}. The coarse fraction of ODP 983 reflects both the delivery of IRD (which increases during stadials) and the input of fine fraction (which decreases during stadials due to reduced advection of fine material to ODP site 983 by slower currents crossing the Iceland-Faeroe ridge [Raymo et al., 2004]).

IRD accumulation rates were calculated from IRD/g and dry bulk accumulation rates, obtained by combining linear sedimentation rates with an estimate for dry bulk density, derived from continuous GRAPE (Gamma-Ray Attenuation Porosity Evaluator [Evans, 1965]) density (ρ_{GRAPE}) measurements calibrated with discrete (index property) measurements of wet and dry bulk density [Jansen et al., 1996]:

$$\text{Dry Bulk Density} = (\rho_{\text{GRAPE}} + 0.17) * 1.5547 - 1.5719 \quad (1)$$

2.2 Changing CO₂ versus surface conditions across the North Atlantic region

For comparisons among datasets, individual records were resampled onto a common timescale with a 200yr time-step. In addition, the record of atmospheric CO₂ [Bereiter et al., 2015] was smoothed using a running mean of 2kyr prior to differentiation (note that this limits our analysis to millennial-scale changes in CO₂). The age model for the CO₂ record is AICC2012 [Veres et al., 2012; Bazin et al., 2013], slightly modified according to method 4 of Parrenin et al. [2012] for determination of gas-ice depth differences (Δdepth) along the EDC ice core by alignment of CH₄ with deuterium isotope maxima. This is considered preferable to model-based estimates of Δdepth in the deeper parts of the ice core.

2.2.1 Defining anomalous conditions

Proxies for surface temperature (%NPS in ODP 983, SST in MD01-2443 [Martrat et al., 2007] and $\delta^{18}\text{O}$ in the NGRIP ice core [NGRIP_members, 2004]) are expressed as an anomaly with respect to background conditions (by subtraction of a 7kyr running mean) in order to isolate millennial-scale variability for comparison to the record of $d\text{CO}_2/dt$. The effect of this operation

is equivalent to the 7kyr ‘orbital filter’ applied in previous studies [Alley *et al.*, 2002; Schmittner *et al.*, 2003; Barker *et al.*, 2011]) and is particularly important in records where millennial-scale variations may be less pronounced than orbital timescale (G-IG) changes. For example in the unfiltered record of Greenland $\delta^{18}\text{O}$ (Fig. 2) the coldest (lowest $\delta^{18}\text{O}$) and warmest (highest $\delta^{18}\text{O}$) quartiles (25% of the time) approximate to glacial and interglacial conditions respectively. Thus even though CO_2 is known to increase during the pronounced (cold) stadials of MIS 3 and the last deglaciation (i.e. H-stadials) this is not reflected by the direct comparison of changing CO_2 with NGRIP $\delta^{18}\text{O}$ (Fig. 3a). In contrast, for the hi-pass filtered record (NGRIP $\delta^{18}\text{O}_{\text{hi}}$) the coldest (lowest $\delta^{18}\text{O}_{\text{hi}}$) and warmest (highest $\delta^{18}\text{O}_{\text{hi}}$) quartiles more closely reflect stadial and interstadial periods respectively (Fig. 2), which better differentiates between intervals of CO_2 increase and decrease. In this case (Fig. 3b), and in agreement with expectations, CO_2 tends to increase during the coldest quartile ($\delta^{18}\text{O}_{\text{hi}}$ class 1) and decrease during the warmest quartile ($\delta^{18}\text{O}_{\text{hi}}$ class 4).

It has been suggested that subtraction of a running mean as described will produce ‘artificial’ millennial-scale scale events during transitions between e.g. glacial and interglacial states. For example, if a shift from a long period of low %NPS to a long period of high %NPS (e.g. that associated with a deglacial transition) occurs within a few hundred years then subtraction of a 7kyr running mean will produce a millennial-scale oscillation (from anomalously cold to anomalously warm) in the calculated anomaly while the raw data show no such feature (merely a step-wise transition from low to high). But this is exactly the definition of anomaly that we intend; it is the anomaly with respect to background conditions (defined here by a 7kyr running mean). To give an analogous example, it is commonly thought that the AMOC experienced a weakening associated with Heinrich events during MIS 3 and the last deglaciation [McManus *et al.*, 2004; Henry *et al.*, 2016]. It can be said that the AMOC was anomalously weak during those events, and we also observe that atmospheric CO_2 tended to increase during those same events [Ahn and Brook, 2008; Marcott *et al.*, 2014]. Now, if a period of weakened AMOC lasted for several thousands of years, then presumably at some point we could no longer consider such conditions as anomalous (since they would represent the ‘new normal’). Furthermore we would probably not expect CO_2 to keep increasing for however long the AMOC remained in a weakened state (at some point we would expect the level of atmospheric CO_2 to reach a new equilibrium). But does this mean therefore that we should not consider as anomalous the period directly following the initial weakening? We contend that we should.. By analogy we argue that the millennial-scale events in the record of %NPS_{hi} are not merely fortuitous artefacts of our numerical procedure but by our definition represent periods of anomalous conditions at the site of ODP 983.

Our specific choice of a 7kyr running mean to isolate millennial-scale variability is guided by previous studies [Alley *et al.*, 2002; Schmittner *et al.*, 2003; Barker *et al.*, 2011] and we suggest that this choice reasonably represents background climate evolution on G-IG timescales. Use of a shorter timescale could be argued for from a purely oceanic perspective (perhaps 1-2kyr or more [Yang and Zhu, 2011; Jansen *et al.*, 2018]) as could a longer timescale to account for complete equilibration of land-based ice sheets (perhaps 10kyr). In Figure S4 we demonstrate the effect of different smoothing windows on the derived record of %NPS_{hi}. Varying the smoothing window from 2 to 10kyr actually produces quite similar results, with the main effect being shorter and more accentuated (with respect to other millennial events) early interglacial anomalies when using a shorter smoothing window (except when a pronounced

millennial-scale event occurs in the un-processed record as in T2, when all records look practically identical). In any case when defining the duration of anomalous conditions at the onset of interglacial periods we employ the records of benthic foraminiferal $\delta^{13}\text{C}$ (from the same site) and $\text{GL}_{\text{T_syn_hi}}$ (derived from the Antarctic ice core record) together with $\% \text{NPS}_{\text{hi}}$ (Fig. S4; Sections 4.1, 4.2).

2.3 $\text{GL}_{\text{T_syn_hi}}$ as a zeroth-order approximation for AMOC strength

The inverse relationship observed between millennial-scale temperature anomalies in the Greenland ice core record (i.e. cold stadials and warm interstadials) and the rate of change of Antarctic temperature has been used to argue for involvement of ocean circulation (specifically the AMOC) in abrupt climate change [Schmittner *et al.*, 2003; Stocker and Johnsen, 2003; Barker *et al.*, 2011]. On the other hand it has also been suggested that the comparatively small contribution of the ocean to the net meridional heat flux makes it unlikely that changes in the AMOC would give rise to major changes in climate and moreover that any reduction in northern oceanic heat transport would be compensated by a corresponding increase in atmospheric transport [Wunsch, 2006]. However, while the Greenland ice core temperature record and its Antarctic surrogate ($\text{GL}_{\text{T_syn_hi}}$, which is the inverse rate of change of the Antarctic temperature record [Barker *et al.*, 2011]) might be poor indicators of meridional heat transport associated with the AMOC, results from a range of climate model experiments (using models with different complexities and a variety of triggering mechanisms) suggest that changes in the strength of the AMOC can ultimately lead to the observed relationship between surface temperature changes in the north and south on millennial timescales [Schmittner *et al.*, 2003; Liu *et al.*, 2009; Zhang *et al.*, 2014; Zhang *et al.*, 2017] (although this is less clear for decadal to centennial timescales [Muir and Fedorov, 2015]). Accordingly we view the record of $\text{GL}_{\text{T_syn_hi}}$ as a zeroth order proxy for anomalies in the strength of AMOC i.e. we interpret a millennial-scale warming (cooling) over Antarctica and corresponding negative (positive) value of $\text{GL}_{\text{T_syn_hi}}$ to reflect a relatively weak (strong) mode of the AMOC. An equilibrium mode of AMOC (not anomalously strong or weak with respect to background conditions) would be reflected by $\text{GL}_{\text{T_syn_hi}}$ remaining close to zero (Antarctica not warming or cooling on a millennial timescale) for a prolonged period such as observed during full interglacial and glacial maxima [Barker *et al.*, 2011]. We therefore infer from Figure 4 that atmospheric CO_2 changes most when the AMOC is not in equilibrium (relatively high absolute values of $\text{GL}_{\text{T_syn_hi}}$). This is in agreement with a range of carbon cycle model simulations [Marchal *et al.*, 1998; Kohler *et al.*, 2005; Menviel *et al.*, 2008; Schmittner and Galbraith, 2008; Menviel *et al.*, 2014; Ganopolski and Brovkin, 2017]. Note again that while our analysis implies that the connection between ocean circulation and CO_2 has remained relatively constant it does not address the specific mechanism involved.

3 Results

3.1 800,000 years of abrupt climate variability

Records of $\% \text{NPS}$, $\% \text{NPS}_{\text{hi}}$ and IRD/g from ODP site 983 are shown in Figure 5. The records show clear glacial-interglacial variability with higher frequency fluctuations throughout the last 800kyr. Wavelet decomposition of the $\% \text{NPS}$ record confirms expectations that

millennial-scale variability is most pronounced during times of intermediate ice volume and transitions between states [McManus *et al.*, 1999; Sima *et al.*, 2004; Barker *et al.*, 2011; Hodell *et al.*, 2015]. It could be argued that the reduction in variance in the millennial band during full glacial and interglacial conditions merely reflects saturation of the %NPS proxy during those times. However, previous interglacials rarely reflect the near zero %NPS values characteristic of modern conditions at this site (Figs. 1, 5). In particular, interglacials before MIS 11 reveal significantly higher levels of %NPS, implying colder conditions reminiscent of the ‘lukewarm interglacials’ observed in Antarctic and deep ocean temperature records as well that of atmospheric CO₂ [Elderfield *et al.*, 2012; PIGS_working_group, 2016]. The fact that %NPS is far from saturation during these earlier interglacials gives us confidence in our assertion that millennial scale variability really is subdued during these periods.

3.2 Changing atmospheric CO₂ and North Atlantic climate over the past 8 glacial cycles

In Figure 6 we show an analysis of the relationship between changing atmospheric CO₂ and North Atlantic surface conditions over the last ~800kyr (Methods Section 2.2). Periods of intense ice rafting *and* high %NPS_{hi} at ODP site 983 (i.e. anomalously cold with respect to background conditions) are dominated by increasing CO₂ (sector X in Fig. 6a, b) whereas CO₂ tends to decrease during intervals of anomalous warmth *and* minimal ice rafting (sector Y in Fig. 6a, b). Note that more than 75% of instances (representing discrete 200yr intervals) within sectors X and Y have positive and negative rates of dCO₂/dt respectively. The distribution of cumulative CO₂ rise and fall with respect to surface conditions at ODP site 983 over the last 800kyr (Fig. 6c, d) is consistent with that observed over the last glacial cycle using either NE Atlantic sea surface temperature (SST) [Martrat *et al.*, 2007] or Greenland ice core δ¹⁸O as a proxy for temperature [NGRIP_members, 2004] (Methods Section 2.2; Fig. 3). Our analysis is insensitive to whether we employ the concentration of IRD (IRD/g) or the accumulation rate (Fig. 6c) because of the large range (6 orders of magnitude) in IRD delivery to the site, which hugely outweighs the effects of changing bulk sedimentation rate on the concentration of IRD. By analogy to the observed relationship between changes in ocean circulation and surface conditions in the North Atlantic region during the last glacial and deglacial periods (Fig. 2) we therefore conclude that the relationship between changing atmospheric CO₂ and ocean circulation as observed over the last glacial cycle [Ahn and Brook, 2008; Marcott *et al.*, 2014; Henry *et al.*, 2016; Deaney *et al.*, 2017] has been relatively invariant over the past 800kyr, as also suggested by the analysis shown in Figure 4.

While our analysis confirms that a major proportion of CO₂ rise over the past 800kyr coincided with cold, icy conditions across the North Atlantic, it does not negate the observation that CO₂ does not always rise when the North Atlantic is cold [Ahn and Brook, 2014]. This is clear from the many instances where CO₂ does not change or even decreases while cold conditions prevail (Figs. 3, 6). In fact from Figure 6 (a, b) it can be seen that anomalously cold intervals at ODP site 983 (%NPS_{hi} class 1) which also have low relative concentrations of IRD (IRD class 3 and 4) display a bias towards decreasing CO₂. The result is that ~25% of cumulative CO₂ fall over the past 800kyr coincides with the coldest quartile at this site (Fig. 6d), which is somewhat at odds with our analysis of the equivalent relationship between dCO₂/dt and NE Atlantic SST or Greenland δ¹⁸O (Fig. 3). Previously [Barker *et al.*, 2015] we showed that surface cooling at site 983 can occur hundreds to thousands of years before the transition to stadial conditions *sensu stricto* and may therefore occur while atmospheric CO₂ is decreasing during a warm Greenland interstadial (thus some of an interstadial decrease in CO₂ effectively ‘leaks’ into

a cold interval at site 983). This would explain why the seemingly anomalous intervals of decreasing CO₂ correspond to intervals of reduced IRD (i.e. during interstadials if defined as periods with low IRD). The effect can be demonstrated by systematically shifting the age assignments of the 983 %NPS_hi record toward younger ages (Fig. 6d). Doing so effectively shifts the cooling transitions so they no longer intersect (to such an extent) with intervals of decreasing CO₂ (i.e. they occur later with respect to the change in CO₂).

Our age model for ODP site 983 is derived by tuning to the ice core record on the AICC2012 age model. Therefore we need to be concerned about the relative errors between our age model and AICC2012 for our comparisons to the record of atmospheric CO₂. Uncertainties in the relative age models of 983 (as determined here) and the CO₂ record derive partly from the precision of tuning between abrupt transitions (of the order of a few hundred years for individual tie points [Barker *et al.*, 2011]) but also from the possibility of choosing the wrong transitions, which is difficult to quantify. We therefore assess the impact of potential uncertainties in the age model by repeating the analyses with systematic shifts in the age assignments of the 983 records (Fig. S5). By applying a systematic shift to the whole record we are greatly exaggerating the likely effect of true errors since we expect a distribution of errors with a mean approximating zero along the 800kyr length of the records. However, even when shifting the age model by 1000yr in either direction the distribution of cumulative CO₂ change versus IRD/g is minimally affected. The largest impact is on the cumulative fall in CO₂ with respect to %NPS_hi (as described above). The relative insensitivity of our analyses to large changes in age assignment is to some extent due to the 2kyr pre-smoothing of the CO₂ record before differentiating. This has the effect of ‘spreading’ the influence of intervals of changing CO₂ beyond their actual limits, which flattens the distribution across classes but also buffers against age model error.

We also compare our age model with that produced for the same core by Lisiecki and Raymo [2005] as part of the LR04 benthic foraminiferal $\delta^{18}\text{O}$ stack (Fig. S5). Note that we did not produce the age model used in this comparison. Use of the LR04 age model necessarily alters the calculated distribution of cumulative CO₂ rise and fall because many millennial-scale oscillations will be completely misaligned. However it does not affect the general relationship observed when using the tuned age model. This probably reflects the fact that the timing of glacial terminations within LR04 is very similar to that implied by the AICC2012 ice core age model (note benthic $\delta^{18}\text{O}$ records in Fig. 7) i.e. the major terminal ice rafting events and corresponding shifts in atmospheric CO₂ are aligned irrespective of the age model employed.

3.3 Glacial terminations at ODP site 983

Glacial terminations at ODP site 983 are characterized by pulses of ice rafting followed by an abrupt warming - a shift from high to low %NPS (Figs. 5 and 7). We interpret these phenomena to reflect early deglacial ice sheet wasting and related freshwater release (in the form of melting icebergs) to the North Atlantic while cold conditions prevail. Once ice rafting ceases the abrupt warming reflects northward migration of the polar front [Zahn, 1994; Barker *et al.*, 2015] (Fig. 1). Our results are consistent with previous studies suggesting a ubiquitous link between abrupt climate shifts and deglaciation [Venz *et al.*, 1999; Cheng *et al.*, 2009; Barker *et al.*, 2011; Cheng *et al.*, 2016] and by analogy with the last two terminations, where direct reconstructions of ocean circulation exist [McManus *et al.*, 2004; Roberts *et al.*, 2010; Böhm *et al.*, 2015; Deaney *et al.*, 2017], we infer that terminal ice rafting events in general are associated with a weakened and or shallow mode of AMOC [see also Venz *et al.*, 1999] with the subsequent

shift to warm, ice-free conditions reflecting recovery of the AMOC and in particular an increased flow of warm Atlantic surface waters into the Norwegian Sea [Lehman and Keigwin, 1992] and corresponding strengthening of the so-called Nordic heat pump [Imbrie *et al.*, 1992]. The term Nordic heat pump describes the transfer of heat across the Greenland-Scotland Ridge via warm surface Atlantic waters entering the Nordic Seas and their return to the deep NE Atlantic as dense overflows across the Greenland-Scotland ridge [Imbrie *et al.*, 1992; Dickson and Brown, 1994]. A strong Nordic heat pump is characteristic of interglacial conditions (Fig. 1) [Imbrie *et al.*, 1992; Berger and Jansen, 1994] whereas a southward shift in the mean latitude of deep water formation (as thought to accompany full glacial conditions [Weber *et al.*, 2007]) would indicate a relative strengthening of the so-called boreal heat pump (characterized by open-ocean convection in the boreal Atlantic) at the expense of the Nordic heat pump [Imbrie *et al.*, 1992] (Fig. 1). Higher bulk sediment accumulation rates observed at ODP site 983 during interglacials [Lisiecki and Raymo, 2005; Barker *et al.*, 2015] provide supporting evidence for stronger Iceland-Scotland overflows (and by extension a stronger Nordic heat pump) during these intervals

4 Discussion

In order to make comparisons among previous interglacials it is necessary to define the beginning and end of these periods [Tzedakis *et al.*, 2012; PIGS_working_group, 2016; Ruddiman *et al.*, 2016; Tzedakis *et al.*, 2017]. In particular, the occurrence of millennial scale features associated with the onset of several past interglacials e.g. within the Antarctic ice core records of temperature and greenhouse gasses (including CO₂), gives rise to considerable ambiguity in defining the onset of interglacial conditions [Masson-Delmotte *et al.*, 2010; PIGS_working_group, 2016]. In the following discussion we consider two alternative definitions for the start of interglacial conditions. The first of these (definition 1) was introduced by Tzedakis *et al.* [2012] and is defined as the last significant bipolar-seesaw oscillation [Stocker and Johnsen, 2003] associated with glacial termination. This corresponds to the end of the Younger-Dryas during T1 and the end of Heinrich Event 11 during T2 [Tzedakis *et al.*, 2012]. In Figure 7 this definition is represented by the transition from blue to pink shaded box for each deglaciation of the last 800kyr. According to our age modelling approach, abrupt deglacial warming at ODP site 983 (implied by strongly decreasing %NPS and the end of major ice rafting) is aligned with the abrupt warming (and strengthening of AMOC) implied by GL_{T_syn_hi} (Methods Section 2.3). Hence warm ‘interglacial’ conditions at ODP site 983 begin in parallel with the onset of interglacial climate according to definition 1. On the other hand there are several lines of evidence which suggest that the residual effects of deglaciation can last for thousands of years beyond this point, which we explore below.

4.1 Delayed equilibration of ocean circulation during an interglacial

Venz and Hodell [1999] noted that deglacial minima in a record of benthic foraminiferal $\delta^{13}\text{C}$ obtained from ODP site 982 (close by site 983) persisted well beyond the end of terminal ice rafting events (recorded at the same site) for several previous interglacials. They interpreted this to reflect a delayed recovery of full interglacial-like circulation beyond the start of some interglacials. We observe the same behaviour at ODP site 983 (Fig. 7); deglacial minima in benthic $\delta^{13}\text{C}$ can persist for thousands of years beyond the end of ice rafting and abrupt warming at this site. Although benthic foraminiferal $\delta^{13}\text{C}$ is not a conservative tracer for circulation (being

sensitive to changes in biology and end-member variability) there are other lines of evidence supporting the assertion that ocean circulation may not recover to its full (quasi-equilibrium) interglacial mode for thousands of years beyond termination. Previous studies across T2, using sedimentary grain size as a proxy for the vigour of one of the main deep water currents crossing the Iceland-Scotland Ridge (Iceland-Scotland Overflow Water, ISOW), have concluded that the production and or density of deep waters formed in the Nordic Seas (a critical component of the modern Nordic heat pump) during the earliest part of the last interglacial period was subdued by continued melting of proximal ice sheets [Hodell *et al.*, 2009; Deaney *et al.*, 2017]. A similar case has been made for the delayed recovery of a modern-like AMOC during the early Holocene [Thornalley *et al.*, 2010; Thornalley *et al.*, 2013].

Masson-Delmotte *et al.* [2010] suggested that early interglacial maxima observed in the Antarctic ice core temperature record are caused by “transient heat transport redistribution comparable with glacial north–south seesaw abrupt climatic changes”. Indeed, the millennial scale cooling observed across Antarctica as these early interglacial maxima subside, gives rise to positive anomalies in the derived record of $GL_{T_syn_hi}$ (implying an anomalously strong mode of AMOC according to our reasoning) that persist for approximately the same duration as the anomalous conditions implied by the record of benthic $\delta^{13}C$ from site 983 (Fig. 7). But how can these records be reconciled? The records of benthic $\delta^{13}C$ and sortable silt seem to imply a ‘weaker’ mode of the Nordic heat pump (at least with respect to full interglacial conditions) during the early part of some interglacials while $GL_{T_syn_hi}$ implies a stronger mode of AMOC. One possibility is that reduced overflow across the Iceland-Scotland ridge (i.e. ISOW) was (more than) compensated by increased transport of deep waters across the Greenland-Iceland ridge (i.e. Denmark Straits Overflow Water, DSOW), resulting in a net strengthening of the Nordic heat pump on its deglacial recovery. On the other hand millennial scale cooling or warming across Antarctica, in response to changes in the AMOC, is most likely insensitive to the location of deep water formation in the North Atlantic. Thus we need only invoke a net strengthening of the North Atlantic heat pump *sensu lato* (the combined Nordic and boreal heat pumps) with respect to equilibrium interglacial conditions in order to reconcile these disparate observations. The potential importance of deep water formation in the subpolar open ocean (i.e., the boreal heat pump) during deglaciation and the onset of abrupt warming events has been suggested by previous modeling studies (e.g. [Knorr and Lohmann, 2007; Barker *et al.*, 2010]).

Building on the model of Broecker and Denton [1989], Imbrie *et al.* [1992; 1993] proposed that the transition from glacial to interglacial state involves a shift from a ‘one-pump’ to a ‘two-pump’ mode. In their model deep water formation in the glacial North Atlantic is limited to the south of Iceland, reflecting a weaker Nordic heat pump and stronger-than-modern boreal heat pump (the ‘one-pump’ mode) with total overturning reduced relative to modern conditions (this inference is qualitatively supported by several model simulations of the glacial AMOC [Weber *et al.*, 2007]). During termination, recovery of the Nordic heat pump occurs while the boreal heat pump is still strong, giving rise to a transient maximum in Atlantic overturning even if the Nordic heat pump does not initially recover to its full interglacial strength (see Fig. 4 in Imbrie *et al.* [1992]). The evidence outlined above seems to provide qualitative support for such a scenario; the shift from negative to positive $GL_{T_syn_hi}$ implies (by our reasoning) a strengthening of AMOC and if our alignment strategy is correct this is paired with a strong warming at the site of ODP 983, which would represent a northerly shift of the polar front and implied strengthening of the Nordic heat pump [Imbrie *et al.*, 1992; Lehman and Keigwin,

1992; *Imbrie et al.*, 1993]. This transition is followed by a period of anomalously strong AMOC (according to $GL_{T_syn_hi}$), which may be accommodated by a stronger-than-modern boreal heat pump even if the Nordic heat pump is not yet up to full interglacial strength (as indicated by the benthic $\delta^{13}C$ and sortable silt data).

Several outstanding issues arise from this discussion, which should be addressed in future studies undertaking more detailed investigations into regional patterns. For example, how do the individual components of AMOC (i.e. ISOW, DSOW and Labrador Sea Water, LSW) contribute to early interglacial changes in AMOC and do they do so in a consistent manner as appears the case for the combined AMOC (as proxied by our records from ODP Site 983). What is the precise mechanism driving the anomalously strong AMOC as proposed during early interglacial time and how is it related to forcing such as insolation, remnant ice-sheets or possible Southern Ocean processes influencing rates of upwelling from the deep ocean?

4.2 Comparing apples and oranges: When is an interglacial not an interglacial?

In our records from ODP site 983 we observe transient maxima in $\%NPS_{hi}$, which resemble the early interglacial maxima in $GL_{T_syn_hi}$, following the end of major deglacial ice rafting events (Fig. 7). We note that typical interglacial values of $\%NPS$ prior to MIS 1 are greater than zero and as such we maintain that this result is not an artefact of proxy saturation. Our analysis suggests that conditions in the NE Atlantic can remain anomalously warm with respect to background conditions for thousands of years after the onset of interglacial conditions according to definition 1. We propose that this reflects the inferred net strengthening of the AMOC (relative to equilibrium interglacial conditions) directly following its deglacial recovery, providing excess heat to the high latitude surface North Atlantic and aiding in the completion of northern hemisphere deglaciation [*Imbrie et al.*, 1992; *Lehman and Keigwin*, 1992; *Imbrie et al.*, 1993]. We note that some early interglacial values of $\%NPS$, which we define as anomalous, are very similar in absolute terms to later values that are not considered anomalous. Again this could be used to argue that the transient early interglacial maxima in $\%NPS_{hi}$ are simply artefacts of our analysis. On the other hand where we have reconstructions of ‘regional’ surface temperature evolution e.g. across T1 and T2, [*Shakun et al.*, 2012; *Hoffman et al.*, 2017] we see that the abrupt warming implied by our record of $\%NPS$ does indeed occur thousands of years before the end of gradual North Atlantic or northern hemisphere warming (Fig. S6) and should thus be considered as anomalous. The local surface temperature evolution at the site of ODP 983 reflects both regional (‘background’) temperature variability of Atlantic surface water masses, superimposed by changes in the transport and mixing of those water masses and although regional reconstructions must also contain both of these signals, the northerly position of ODP site 983 makes it particularly sensitive to changes in circulation.

Given the different lines of evidence for anomalous (non-equilibrium) conditions lasting beyond the start of an interglacial according to definition 1, we propose a second definition (definition 2) for the onset of quasi-equilibrium interglacial conditions that coincides with the end of this anomalous phase as expressed by $\%NPS_{hi}$, benthic $\delta^{13}C$ and $GL_{T_syn_hi}$ (the end of the pink box in Fig. 7). In several cases this definition could be extended to encompass secondary features but we limit our description to include only the major features. Note that our aim is not to reinvent the definition of an interglacial but rather to highlight the complexities introduced by non-equilibrium conditions when making comparisons among different

interglacials. In this respect we are reiterating earlier warnings [e.g. *Masson-Delmotte et al.*, 2010; *PIGS_working_group*, 2016]. Below we investigate the implications of this complexity for investigations into the interglacial evolution of atmospheric CO₂.

In Figure S7 we plot the coevolution of benthic $\delta^{18}\text{O}$ (a crude proxy for global ice volume) versus atmospheric CO₂ for the last 8 glacial cycles. Although the records are on independent age models (LR04 versus AICC2012) a deglacial lead of increasing CO₂ ahead of decreasing ice volume is discernable for the majority of cases (note the exceptions T6 and T8 will be discussed later). This was demonstrated with greater precision in a study by *Shackleton* [2000] and conveniently conveys the importance of rising CO₂ as a critical ingredient in the deglacial process [*Broecker and Denton*, 1989; *Imbrie et al.*, 1993; *Shakun et al.*, 2012]. The coloured symbols in Figure 8 (a, b) represent the coevolution of benthic $\delta^{18}\text{O}$ and CO₂ across the last 9 glacial terminations using the first and second definitions respectively for the onset of interglacial conditions (i.e. across the blue or blue and pink boxes combined in Fig. 7). It is unsurprising that use of definition 2 encompasses a more complete transition with respect to benthic $\delta^{18}\text{O}$ as compared with definition 1; on orbital timescales ice volume typically responds later than other climatic indicators [*Shackleton*, 2000], for example during the most recent deglaciation sea level continued to rise until at least 8ka, well beyond the conventional start of the Holocene interglacial [*Smith et al.*, 2011].

On the other hand, the main phase of deglacial CO₂ rise typically occurs prior to the onset of interglacial conditions irrespective of which definition is used i.e. most of the rise in CO₂ takes place within the blue boxes in Figure 7. Of particular relevance though are several instances (T1, T3b, T4, T9) where use of definition 2 incorporates an interval of decreasing CO₂ prior to the implied onset of equilibrium interglacial conditions (Fig. 8b). These phases of decreasing CO₂ correspond to particularly warm (low %NPS) and relatively ice-free (low IRD/g) conditions at the site of ODP 983 (Fig 8d, f). In fact several terminations (including T3b, T4 and T9; Fig. 8h) extend into sector Y in Figure 6a, b; conditions that are typically associated with decreasing atmospheric CO₂. Notably, terminations T3b, T4 and T9 reveal higher rates of CO₂ decrease during their early ‘non-equilibrium’ interglacial sections than any other deglaciation of the past 800kyr. These terminations also correspond to MIS 7, 9 and 19, which were identified by *Ruddiman et al.* [2016] as those interglacials most consistently associated with a decreasing trend in atmospheric CO₂. We believe that our observation of a systematic link between changing CO₂ and non-equilibrium oceanic conditions during the early phase of several previous interglacials provides a strong basis for concluding that this link is causal i.e. that an early interglacial decrease in atmospheric CO₂ is most likely a direct consequence of a non-equilibrium ocean state. Such an inference is in line with transient carbon cycle modelling studies which consistently imply that CO₂ will change whenever ocean circulation is not in equilibrium [*Marchal et al.*, 1998; *Kohler et al.*, 2005; *Menviel et al.*, 2008; *Schmittner and Galbraith*, 2008; *Menviel et al.*, 2014; *Ganopolski and Brovkin*, 2017].

We therefore suggest that the early interglacial intervals we identify as anomalous (Figs. 5, 7) should not be counted in any survey of interglacial trends where quasi-equilibrium conditions may be assumed; for these purposes such intervals should be considered as a part of the deglacial process. For example, the highest interglacial values of CO₂ during MIS 5, 7, 9 and 19 occur within the intervals we identify as anomalous (the pink boxes in Figs. 5 and 7). If these intervals were not included in the analysis of interglacial CO₂ it is unclear that such a consistent

decreasing trend in CO₂ would be identified for these particular interglacials. Thus while we are not commenting on the overall conclusions of *Ruddiman et al.* [2016] our findings do suggest that some reevaluation may be required. We stress again that we are not trying to redefine what an interglacial is and we do not consider definition 2 as a ‘better’ definition of when an interglacial begins. Here we are concerned with the legacy of deglacial instabilities, which we suggest can last for thousands of years after the beginning of an interglacial as traditionally defined.

As to why some interglacials experience more pronounced overshoots in CO₂ than others, we concur with earlier studies [*Deaney et al.*, 2017; *Ganopolski and Brovkin*, 2017] which suggest this might be related to the timing of AMOC recovery with respect to deglaciation; If recovery occurs midway through the termination (e.g. with the Bølling-Allerød during T1) then we might expect a smaller overshoot than for a termination where AMOC recovery occurs only towards the end (e.g. T2). The case of T3b is an interesting one (Fig. 7); the records of %NPS_{hi} and GL_{T_syn} suggest that the AMOC might have made an early recovery (albeit a partial one considering the small decrease in %NPS) ~250ka and yet we observe a large overshoot in CO₂ at the end of termination ~243ka. Recovery of the AMOC during deglaciation may occur with the cessation of freshwater release across the North Atlantic [*Liu et al.*, 2009; *Ganopolski and Brovkin*, 2017] or in response to more gradual global warming, in which case the addition of freshwater may still act to delay resumption [*Knorr and Lohmann*, 2007]. Future studies should focus on the interplay between these parameters when considering individual terminations.

4.3 Protracted terminations: T6, T8 (and T5?)

Tzedakis et al. [2017] formulated a simple rule for predicting the occurrence of interglacials as a function of integrated northern summer insolation. Their predictions provide insight into some of the atypical behaviour we observe associated with a number of terminations. For example, the warming transitions (shift from high to low %NPS) following the major deglacial pulses of ice rafting associated with T6 (leading to MIS 13; Fig. 7) and T8 (leading to MIS 17) are not particularly abrupt or pronounced. In fact these terminations end with the least anomalous values of %NPS_{hi} (out of all the deglacial transitions covered here) and are followed by further pulses of ice rafting while warming continues. Hence we label these transitions protracted terminations. We note that both T6 and T8 are associated with insolation peaks that do not pass the Tzedakis test (i.e. they do not cross the threshold for producing an interglacial state according to that study; Fig. 5), even though subsequent peaks allow for inclusion of MIS 13 and MIS 17 within the set of Late Pleistocene interglacials. We note also that the cycles of benthic $\delta^{18}\text{O}$ versus atmospheric CO₂ from MIS 15 to 13 and from MIS 19 to 17 (Fig. S7) do not show the same apparent hysteresis as other cycles. The deglacial rise in CO₂ across T6 (and to a lesser extent across T8) does not lead the initial decrease in $\delta^{18}\text{O}$ (ice volume) and CO₂ continues to increase gradually throughout deglaciation. The formulation presented by *Tzedakis et al.* [2017] utilises a discount applied to the threshold required to generate an interglacial, which depends on the time since the threshold was last crossed. Implicit in their argument is the existence of a component within the climate system that is capable of storing the potential ‘energy’ (or equivalent) required to amplify a modest increase in summer insolation and produce a glacial termination. Crucially, for T6 and T8, this component must not

lose its (full) potential during the initial phase of deglaciation (which occurs much earlier than the insolation peak that eventually passes the Tzedakis test). Our results suggest that T6 and T8 were atypical in that changes across them were less pronounced than other terminations. We note that for T8, atmospheric CO₂ continued to rise (albeit only on average) until the threshold was crossed but T6 was more complicated. We also note that the insolation peak associated with T5 (leading into MIS 11) comprises two precession peaks and it is only the second of these (in combination with high obliquity) that exceeds the threshold for an interglacial. Perhaps this could help to explain why the transition from MIS 12 into MIS 11 also appears somewhat protracted (Fig. 5) as described by *Rohling et al.* [2010].

4.4 The ‘non-uniqueness’ of Heinrich events

Heinrich [1988] and *Bond et al.* [1992] described a series of detrital layers deposited across the mid-latitude North Atlantic. These layers of ice rafted debris were proposed to reflect episodic collapses of the Laurentide ice sheet (‘Heinrich events’) with icebergs being discharged through the Hudson Strait providing meltwater to large portions of the surface North Atlantic. The longest [*NGRIP_members*, 2004] and coldest [*Shackleton et al.*, 2000; *Martrat et al.*, 2007] stadial events recorded across the North Atlantic region during MIS 3 were associated with H-events and these have been termed Heinrich-stadials [*Skinner and Elderfield*, 2007; *Barker et al.*, 2009]. The large volume of freshwater release associated with H-events [*Hemming*, 2004] is thought to have affected ocean circulation and empirical evidence suggests that H-stadials were associated with particularly strong perturbations of the AMOC as compared with non-H stadials [*Piotrowski et al.*, 2005; *Henry et al.*, 2016]. The H-stadials of MIS 3 were also associated with much larger increases in atmospheric CO₂ than the smaller non-H stadials [*Ahn and Brook*, 2008; *Ahn and Brook*, 2014]. Thus Heinrich events themselves have become synonymous with extreme perturbations of the AMOC and rising atmospheric CO₂. On the other hand it is not clear whether H-events were the primary cause of such perturbations [*Bond and Lotti*, 1995; *Shaffer et al.*, 2004; *Alvarez-Solas et al.*, 2013; *Barker et al.*, 2015]. Furthermore a number of studies provide evidence that Heinrich events *sensu stricto* (i.e. sourced from Hudson Strait) first appeared around 640ka [*Hodell et al.*, 2008; *Naafs et al.*, 2011] but we do not observe any systematic change in the relationship between surface conditions and changing atmospheric CO₂ across this interval (Fig. S8), suggesting that the observed correlation between Heinrich events *sensu stricto* and millennial-scale changes in atmospheric CO₂ during the last glacial cycle does not necessarily reflect a causal link. We propose therefore that the massive Hudson Strait ice discharge events were not unique in terms of their potential impact on ocean circulation and atmospheric CO₂, allowing for the possibility that another source of freshwater or alternative mechanism might play an important role.

5 Conclusions

We have presented continuous proxy records of NE Atlantic surface conditions spanning the past 800kyr, encompassing 8 glacial cycles and 9 glacial terminations. Our records confirm that the occurrence of millennial-scale variability throughout this period was most pronounced during times of intermediate ice volume and transitions between glacial and interglacial state. Our results reveal a link between surface ocean conditions and changes in atmospheric CO₂ that

is consistent with independent observations and reconstructions over the last glacial cycle and we therefore infer that the hypothesized mechanistic link between ocean circulation and CO₂ (with CO₂ rising on a millennial-timescale when Atlantic circulation is in a weakened state and vice versa) has been maintained throughout the last 800kyr.

According to our reconstructions, glacial terminations are characterized by a prolonged interval of cold, icy conditions across the high latitude North Atlantic during which atmospheric CO₂ rises and (by our reasoning) the AMOC is in a weakened state. Subsequent and abrupt warming occurs with the end of iceberg discharge, and is followed by an interval of anomalous warmth, during which CO₂ may decrease again before reaching its equilibrium interglacial concentration. We interpret this sequence of events to reflect the recovery and amplification of AMOC during early interglacial times when we infer there to be a stronger-than-modern boreal heat pump in combination with a strong, or strengthening, Nordic heat pump. We therefore suggest that the evolution of atmospheric CO₂ during these periods reflects non-equilibrium conditions (i.e. the climate system has not yet re-equilibrated following deglaciation) and should not be considered within comparisons among interglacials. A number of deglaciations (in particular Terminations 6 and 8 and potentially T5) do not follow the typical trend, with less pronounced warming and multiple phases of ice rafting. These deglaciations also experienced weaker insolation forcing than is considered requisite to give rise to interglacial conditions and we label these as protracted terminations. Finally, we note that the observed relationship between surface ocean conditions and changing CO₂ did not change with the onset of Heinrich events sourced from the Hudson Strait ~640ka. We therefore conclude that Heinrich events *sensu stricto* were not unique in terms of their potential impact on ocean circulation and atmospheric CO₂, sustaining the question as to the precise drivers of large scale perturbations of the AMOC and corresponding variations in CO₂.

Acknowledgments

We thank the Editor, Luke Skinner and two anonymous reviewers for their careful and constructive evaluations of our study. This research used samples provided by the Integrated Ocean Drilling Program (IODP). We acknowledge support from UK NERC (grants NE/J008133/1, NE/P000878/1 and NE/L006405/1). Author contributions: SB designed project and analysed datasets; SC, SL and DN performed all laboratory work. All authors contributed to writing the paper. The authors declare no competing interests. All data presented here are available in a supplementary data file and online in the PANGAEA data repository: <https://issues.pangaea.de/browse/PDI-21239>.

References

- Ahn, J., and E. J. Brook (2008), Atmospheric CO₂ and climate on millennial time scales during the last glacial period, *Science*, 322(5898), 83-85.
- Ahn, J., and E. J. Brook (2014), Siple Dome ice reveals two modes of millennial CO₂ change during the last ice age, *Nat. Commun.*, 5.

- Alley, R. B., E. J. Brook, and S. Anandakrishnan (2002), A northern lead in the orbital band: north-south phasing of Ice-Age events, *Quat. Sci. Rev.*, 21(1-3), 431-441.
- Alvarez-Solas, J., A. Robinson, M. Montoya, and C. Ritz (2013), Iceberg discharges of the last glacial period driven by oceanic circulation changes, *Proc. Natl. Acad. Sci.*, 110(41), 16350-16354.
- Anderson, R. F., S. Ali, L. I. Bradtmiller, S. H. H. Nielsen, M. Q. Fleisher, B. E. Anderson, and L. H. Burckle (2009), Wind-driven upwelling in the Southern Ocean and the deglacial rise in atmospheric CO₂, *Science*, 323(5920), 1443-1448.
- Barker, S., G. Knorr, M. Vautravers, P. Diz, and L. C. Skinner (2010), Extreme deepening of the Atlantic overturning circulation during deglaciation, *Nat. Geosci.*, 3, 567-571 doi: 510.1038/NGEO1921.
- Barker, S., J. Chen, X. Gong, L. Jonkers, G. Knorr, and D. Thornalley (2015), Icebergs not the trigger for North Atlantic cold events, *Nature*, 520(7547), 333-336.
- Barker, S., P. Diz, M. J. Vautravers, J. Pike, G. Knorr, I. R. Hall, and W. S. Broecker (2009), Interhemispheric Atlantic seesaw response during the last deglaciation, *Nature*, 457(7233), 1097-1102.
- Barker, S., G. Knorr, R. L. Edwards, F. Parrenin, A. E. Putnam, L. C. Skinner, E. Wolff, and M. Ziegler (2011), 800,000 years of abrupt climate variability, *Science*, 334(6054), 347-351.
- Bazin, L., A. Landais, B. Lemieux-Dudon, H. Toyé Mahamadou Kele, D. Veres, F. Parrenin, P. Martinerie, C. Ritz, E. Capron, and V. Lipenkov (2013), An optimized multi-proxy, multi-site Antarctic ice and gas orbital chronology (AICC2012): 120-800 ka, *Clim. Past*, 9(4), 1715-1731.
- Bereiter, B., S. Eggelston, J. Schmitt, C. Nehrbass-Ahles, T. F. Stocker, H. Fischer, S. Kipfstuhl, and J. Chappellaz (2015), Revision of the EPICA Dome C CO₂ record from 800 to 600 kyr before present, *Geophys. Res. Lett.*, 42(2), 542-549.
- Berger, W. H., and E. Jansen (1994), Mid-pleistocene climate shift-the Nansen connection, *The polar oceans and their role in shaping the global environment*, 295-311.
- Böhm, E., J. Lippold, M. Gutjahr, M. Frank, P. Blaser, B. Antz, J. Fohlmeister, N. Frank, M. Andersen, and M. Deininger (2015), Strong and deep Atlantic meridional overturning circulation during the last glacial cycle, *Nature*, 517(7532), 73-76.
- Bond, G., et al. (1992), Evidence for massive discharges of icebergs into the north Atlantic Ocean during the Last Glacial Period, *Nature*, 360(6401), 245-249.
- Bond, G. C., and R. Lotti (1995), Iceberg Discharges into the North-Atlantic on Millennial Time Scales During the Last Glaciation, *Science*, 267(5200), 1005-1010.
- Broecker, W. S., and J. van Donk (1970), Insolation changes, ice volumes and the O¹⁸ in deep-sea cores, *Rev. Geophys. Space Phys.*, 8(1), 169-198.
- Broecker, W. S., and G. H. Denton (1989), The role of ocean-atmosphere reorganizations in glacial cycles, *Geochim. Cosmochim. Acta*, 53(10), 2465-2501.
- Broecker, W. S., J. Lynch-Stieglitz, E. Clark, I. Hajdas, and G. Bonani (2001), What caused the atmosphere's CO₂ content to rise during the last 8000 years?, *Geochemistry Geophysics Geosystems*, 2, U1-U13.
- Caesar, L., S. Rahmstorf, A. Robinson, G. Feulner, and V. Saba (2018), Observed fingerprint of a weakening Atlantic Ocean overturning circulation, *Nature*, 556(7700), 191.
- Channell, J. E. T., D. A. Hodell, and B. Lehman (1997), Relative geomagnetic paleointensity and delta O-18 at ODP Site 983 (Gardar Drift, North Atlantic) since 350 ka, *Earth Planet. Sci. Lett.*, 153(1-2), 103-118.
- Chen, T., L. F. Robinson, A. Burke, J. Southon, P. Spooner, P. J. Morris, and H. C. Ng (2015), Synchronous centennial abrupt events in the ocean and atmosphere during the last deglaciation, *Science*, 349(6255), 1537-1541.
- Cheng, H., R. L. Edwards, W. S. Broecker, G. H. Denton, X. G. Kong, Y. J. Wang, R. Zhang, and X. F. Wang (2009), Ice Age Terminations, *Science*, 326(5950), 248-252.
- Cheng, H., R. L. Edwards, A. Sinha, C. Spötl, L. Yi, S. Chen, M. Kelly, G. Kathayat, X. Wang, and X. Li (2016), The Asian monsoon over the past 640,000 years and ice age terminations, *Nature*, 534(7609), 640-646.
- Deaney, E. D., S. Barker, and T. Van de Flierdt (2017), Timing and nature of AMOC recovery across Termination 2 and magnitude of deglacial CO₂ change, *Nat. Commun.*, DOI: 10.1038/NCOMMS14595.
- Denton, G. H., R. F. Anderson, J. R. Toggweiler, R. L. Edwards, J. M. Schaefer, and A. E. Putnam (2010), The Last Glacial Termination, *Science*, 328(5986), 1652-1656.
- Dickson, R. R., and J. Brown (1994), The Production of North-Atlantic Deep-Water - Sources, Rates, and Pathways, *Journal of Geophysical Research-Oceans*, 99(C6), 12319-12341.
- Dima, M., and G. Lohmann (2010), Evidence for two distinct modes of large-scale ocean circulation changes over the last century, *J. Clim.*, 23(1), 5-16.

- Elderfield, H., P. Ferretti, M. Greaves, S. Crowhurst, I. N. McCave, D. Hodell, and A. M. Piotrowski (2012), Evolution of Ocean Temperature and Ice Volume Through the Mid-Pleistocene Climate Transition, *Science*, 337(6095), 704-709.
- Elsig, J., J. Schmitt, D. Leuenberger, R. Schneider, M. Eyer, M. Leuenberger, F. Joos, H. Fischer, and T. F. Stocker (2009), Stable isotope constraints on Holocene carbon cycle changes from an Antarctic ice core, *Nature*, 461(7263), 507.
- Evans, H. B. (1965), GRAPE*-A Device for Continuous Determination of Material Density and Porosity, paper presented at SPWLA 6th Annual Logging Symposium (Volume II), Society of Petrophysicists and Well-Log Analysts.
- Eynaud, F. (2011), Planktonic foraminifera in the Arctic: potentials and issues regarding modern and quaternary populations, *IOP Conference Series: Earth and Environmental Science*, 14(1), 012005.
- Ezat, M. M., T. L. Rasmussen, and J. Groeneveld (2014), Persistent intermediate water warming during cold stadials in the southeastern Nordic seas during the past 65 k.y., *Geology*, doi: 10.1130/G35579.1.
- Ganopolski, A., and V. Brovkin (2017), Simulation of climate, ice sheets and CO₂ evolution during the last four glacial cycles with an Earth system model of intermediate complexity, *Clim. Past*, 13(12), 1695.
- Grinsted, A., J. C. Moore, and S. Jevrejeva (2004), Application of the cross wavelet transform and wavelet coherence to geophysical time series, *Nonlinear Process. Geophys.*, 11(5/6), 561-566.
- Heinrich, H. (1988), Origin and consequences of cyclic ice rafting in the Northeast Atlantic Ocean during the past 130,000 years, *Quat. Res.*, 29(2), 142-152.
- Hemming, S. R. (2004), Heinrich events: Massive late pleistocene detritus layers of the North Atlantic and their global climate imprint, *Rev. Geophys.*, 42(1).
- Henry, L., J. F. McManus, W. B. Curry, N. L. Roberts, A. M. Piotrowski, and L. D. Keigwin (2016), North Atlantic ocean circulation and abrupt climate change during the last glaciation, *Science*, 353(6298), 470-474.
- Hodell, D., L. Lourens, S. Crowhurst, T. Konijnendijk, R. Tjallingii, F. Jiménez-Espejo, L. Skinner, P. Tzedakis, and S. S. P. Members (2015), A reference time scale for Site U1385 (Shackleton Site) on the SW Iberian Margin, *Global Planet. Change*, 133, 49-64.
- Hodell, D. A., J. E. T. Channell, J. H. Curtis, O. E. Romero, and U. Roehl (2008), Onset of "Hudson Strait" Heinrich events in the eastern North Atlantic at the end of the middle Pleistocene transition (similar to 640 ka)?, *Paleoceanography*, 23(4).
- Hodell, D. A., E. K. Minth, J. H. Curtis, I. N. McCave, I. R. Hall, J. E. T. Channell, and C. Xuan (2009), Surface and deep-water hydrography on Gardar Drift (Iceland Basin) during the last interglacial period, *Earth Planet. Sci. Lett.*, 288(1-2), 10-19.
- Hoffman, J. S., P. U. Clark, A. C. Parnell, and F. He (2017), Regional and global sea-surface temperatures during the last interglaciation, *Science*, 355(6322), 276-279.
- Imbrie, J., et al. (1992), On the Structure and Origin of Major Glaciation Cycles 1. Linear responses to Milankovitch forcing, *Paleoceanography*, 7(6), 701-738.
- Imbrie, J., et al. (1993), On the structure and origin of major glaciation cycles 2. the 100,000-year cycle, *Paleoceanography*, 8(6), 699-735.
- Indermuhle, A., et al. (1999), Holocene carbon-cycle dynamics based on CO₂ trapped in ice at Taylor Dome, Antarctica, *Nature*, 398(6723), 121-126.
- Jansen, E., M. E. Raymo, and P. Blum (1996), *Proceedings of the Ocean Drilling Program, Initial Reports. Vol. 162*, Texas A & M University, Ocean Drilling Program.
- Jansen, M. F., L. P. Nadeau, and T. M. Merlis (2018), Transient versus Equilibrium Response of the Ocean's Overturning Circulation to Warming, *J. Clim.*, 31(13), 5147-5163, doi: 10.1175/jcli-d-17-0797.1.
- Jouzel, J., et al. (2007), Orbital and millennial Antarctic climate variability over the past 800,000 years, *Science*, 317(5839), 793-796.
- Kleinen, T., V. Brovkin, W. von Bloh, D. Archer, and G. Munhoven (2010), Holocene carbon cycle dynamics, *Geophys. Res. Lett.*, 37(2).
- Kleiven, H. F., I. R. Hall, I. N. McCave, G. Knorr, and E. Jansen (2011), Coupled deep-water flow and climate variability in the middle Pleistocene North Atlantic, *Geology*, 39(4), 343-346.
- Knorr, G., and G. Lohmann (2007), Rapid transitions in the Atlantic thermohaline circulation triggered by global warming and meltwater during the last deglaciation, *Geochem. Geophys. Geosyst.*, 8, DOI:10.1029/2007GC001604.
- Kohler, P., H. Fischer, G. Munhoven, and R. E. Zeebe (2005), Quantitative interpretation of atmospheric carbon records over the last glacial termination, *Global Biogeochem. Cycles*, 19(4).

- Lehman, S. J., and L. D. Keigwin (1992), Sudden changes in North Atlantic circulation during the last deglaciation, *Nature*, 356(6372), 757-762.
- Lisiecki, L. E., and M. E. Raymo (2005), A Pliocene-Pleistocene stack of 57 globally distributed benthic $\delta^{18}\text{O}$ records, *Paleoceanography*, 20(2), DOI:10.1029/2004PA001071.
- Liu, Z., et al. (2009), Transient Simulation of Last Deglaciation with a New Mechanism for Bolling-Allerod Warming, *Science*, 325(5938), 310-314.
- Loulergue, L., A. Schilt, R. Spahni, V. Masson-Delmotte, T. Blunier, B. Lemieux, J. M. Barnola, D. Raynaud, T. F. Stocker, and J. Chappellaz (2008), Orbital and millennial-scale features of atmospheric CH_4 over the past 800,000 years, *Nature*, 453(7193), 383-386.
- Marchal, O., T. F. Stocker, and F. Joos (1998), Impact of oceanic reorganizations on the ocean carbon cycle and atmospheric carbon dioxide content, *Paleoceanography*, 13(3), 225-244.
- Marcott, S. A., T. K. Bauska, C. Buizert, E. J. Steig, J. L. Rosen, K. M. Cuffey, T. Fudge, J. P. Severinghaus, J. Ahn, and M. L. Kalk (2014), Centennial-scale changes in the global carbon cycle during the last deglaciation, *Nature*, 514(7524), 616-619.
- Margo_Project_Members (2009), Constraints on the magnitude and patterns of ocean cooling at the Last Glacial Maximum, *Nat. Geosci.*, 2(2), 127-132.
- Martrat, B., J. O. Grimalt, N. J. Shackleton, L. de Abreu, M. A. Hutterli, and T. F. Stocker (2007), Four climate cycles of recurring deep and surface water destabilizations on the Iberian margin, *Science*, 317(5837), 502-507.
- Masson-Delmotte, V., B. Stenni, K. Pol, P. Braconnot, O. Cattani, S. Falourd, M. Kageyama, J. Jouzel, A. Landais, and B. Minster (2010), EPICA Dome C record of glacial and interglacial intensities, *Quat. Sci. Rev.*, 29(1), 113-128.
- McManus, J. F., D. W. Oppo, and J. L. Cullen (1999), A 0.5-million-year record of millennial-scale climate variability in the North Atlantic, *Science*, 283(5404), 971-975.
- McManus, J. F., R. Francois, J. M. Gherardi, L. D. Keigwin, and S. Brown-Leger (2004), Collapse and rapid resumption of Atlantic meridional circulation linked to deglacial climate changes, *Nature*, 428(6985), 834-837.
- Menviel, L., A. Timmermann, A. Mouchet, and O. Timm (2008), Meridional reorganizations of marine and terrestrial productivity during Heinrich events, *Paleoceanography*, 23(1), DOI:10.1029/2007PA001445.
- Menviel, L., M. H. England, K. Meissner, A. Mouchet, and J. Yu (2014), Atlantic-Pacific seesaw and its role in outgassing CO_2 during Heinrich events, *Paleoceanography*, 29(1), 58-70.
- Milankovitch, M. (1941), *Kanon der Erdbestrahlung und seine Anwendung auf das Eiszeiten-problem*, Royal Serbian Academy, Belgrade.
- Muir, L., and A. Fedorov (2015), How the AMOC affects ocean temperatures on decadal to centennial timescales: the North Atlantic versus an interhemispheric seesaw, *Clim. Dyn.*, 45(1-2), 151-160.
- Naafs, B. D. A., J. Hefter, P. Ferretti, R. Stein, and G. H. Haug (2011), Sea surface temperatures did not control the first occurrence of Hudson Strait Heinrich Events during MIS 16, *Paleoceanography*, 26(4).
- NGRIP_members (2004), High-resolution record of Northern Hemisphere climate extending into the last interglacial period, *Nature*, 431(7005), 147-151.
- Oppo, D. W., J. F. McManus, and J. L. Cullen (1998), Abrupt climate events 500,000 to 340,000 years ago: Evidence from subpolar north Atlantic sediments, *Science*, 279(5355), 1335-1338.
- Parrenin, F., S. Barker, T. Blunier, J. Chappellaz, J. Jouzel, A. Landais, V. Masson-Delmotte, J. Schwander, and D. Veres (2012), On the gas-ice depth difference (Δdepth) along the EPICA Dome C ice core, *Clim. Past*, 8, 1239-1255, doi: DOI:10.5194/cp-8-1239-2012.
- PIGS_working_group (2016), Interglacials of the last 800,000 years.
- Piotrowski, A. M., S. L. Goldstein, S. R. Hemming, and R. G. Fairbanks (2005), Temporal relationships of carbon cycling and ocean circulation at glacial boundaries, *Science*, 307(5717), 1933-1938.
- Rahmstorf, S., J. E. Box, G. Feulner, M. E. Mann, A. Robinson, S. Rutherford, and E. J. Schaffernicht (2015), Exceptional twentieth-century slowdown in Atlantic Ocean overturning circulation, *Nature climate change*, 5(5), 475.
- Raymo, M. E., D. W. Oppo, B. P. Flower, D. A. Hodell, J. F. McManus, K. A. Venz, K. F. Kleiven, and K. McIntyre (2004), Stability of North Atlantic water masses in face of pronounced climate variability during the Pleistocene, *Paleoceanography*, 19(2), PA2008, doi:10.1029/2003PA000921.
- Ridgwell, A. J., A. J. Watson, M. A. Maslin, and J. O. Kaplan (2003), Implications of coral reef buildup for the controls on atmospheric CO_2 since the Last Glacial Maximum, *Paleoceanography*, 18(4).

- Roberts, N. L., A. M. Piotrowski, J. F. McManus, and L. D. Keigwin (2010), Synchronous Deglacial Overturning and Water Mass Source Changes, *Science*, 327(5961), 75-78.
- Rohling, E. J., K. Braun, K. Grant, M. Kucera, A. Roberts, M. Siddall, and G. Trommer (2010), Comparison between Holocene and Marine Isotope Stage-11 sea-level histories, *Earth Planet. Sci. Lett.*, 291(1), 97-105.
- Ruddiman, W., D. Fuller, J. Kutzbach, P. Tzedakis, J. Kaplan, E. Ellis, S. Vavrus, C. Roberts, R. Fyfe, and F. He (2016), Late Holocene climate: Natural or anthropogenic?, *Rev. Geophys.*, 54(1), 93-118.
- Ruddiman, W. F. (2003), The anthropogenic greenhouse era began thousands of years ago, *Clim. Change*, 61(3), 261-293.
- Schlitzer, R. (2014), Ocean Data View, <http://odv.awi.de>.
- Schmittner, A., and E. D. Galbraith (2008), Glacial greenhouse-gas fluctuations controlled by ocean circulation changes, *Nature*, 456(7220), 373-376.
- Schmittner, A., O. A. Saenko, and A. J. Weaver (2003), Coupling of the hemispheres in observations and simulations of glacial climate change, *Quat. Sci. Rev.*, 22(5-7), 659-671.
- Shackleton, N. J. (2000), The 100,000-year ice-age cycle identified and found to lag temperature, carbon dioxide, and orbital eccentricity, *Science*, 289(5486), 1897-1902.
- Shackleton, N. J., M. A. Hall, and E. Vincent (2000), Phase relationships between millennial-scale events 64,000-24,000 years ago, *Paleoceanography*, 15(6), 565-569.
- Shaffer, G., S. M. Olsen, and C. J. Bjerrum (2004), Ocean subsurface warming as a mechanism for coupling Dansgaard-Oeschger climate cycles and ice-rafter events, *Geophys. Res. Lett.*, 31(24).
- Shakun, J. D., P. U. Clark, F. He, S. A. Marcott, A. C. Mix, Z. Liu, B. Otto-Bliesner, A. Schmittner, and E. Bard (2012), Global warming preceded by increasing carbon dioxide concentrations during the last deglaciation, *Nature*, 484(7392), 49-54.
- Sigman, D. M., M. P. Hain, and G. H. Haug (2010), The polar ocean and glacial cycles in atmospheric CO₂ concentration, *Nature*, 466(7302), 47-55.
- Sima, A., A. Paul, and M. Schulz (2004), The Younger Dryas - an intrinsic feature of late Pleistocene climate change at millennial timescales, *Earth Planet. Sci. Lett.*, 222(3-4), 741-750.
- Skinner, L., and H. Elderfield (2007), Rapid fluctuations in the deep North Atlantic heat budget during the last glacial period, *Paleoceanography*, 22(1).
- Skinner, L. C., S. Fallon, C. Waelbroeck, E. Michel, and S. Barker (2010), Ventilation of the deep Southern Ocean and deglacial CO₂ rise, *Science*, 328(5982), 1147-1151.
- Smeed, D., S. Josey, C. Beaulieu, W. Johns, B. Moat, E. Frajka-Williams, D. Rayner, C. Meinen, M. Baringer, and H. Bryden (2018), The North Atlantic Ocean is in a state of reduced overturning, *Geophys. Res. Lett.*, 45(3), 1527-1533.
- Smith, D., S. Harrison, C. R. Firth, and J. T. Jordan (2011), The early Holocene sea level rise, *Quat. Sci. Rev.*, 30(15-16), 1846-1860.
- Stocker, T. F., and S. J. Johnsen (2003), A minimum thermodynamic model for the bipolar seesaw, *Paleoceanography*, 18(4), DOI:10.1029/2003PA000920.
- Thornalley, D. J., M. Blaschek, F. J. Davies, S. Praetorius, D. W. Oppo, J. F. McManus, I. R. Hall, H. F. Kleiven, H. Renssen, and I. N. McCave (2013), Long-term variations in Iceland–Scotland overflow strength during the Holocene.
- Thornalley, D. J., D. W. Oppo, P. Ortega, J. I. Robson, C. M. Brierley, R. Davis, I. R. Hall, P. Moffa-Sanchez, N. L. Rose, and P. T. Spooner (2018), Anomalously weak Labrador Sea convection and Atlantic overturning during the past 150 years, *Nature*, 556(7700), 227.
- Thornalley, D. J. R., H. Elderfield, and I. N. McCave (2010), Intermediate and deep water paleoceanography of the northern North Atlantic over the past 21,000 years, *Paleoceanography*, 25, PA1211.
- Tzedakis, P., M. Crucifix, T. Mitsui, and E. W. Wolff (2017), A simple rule to determine which insolation cycles lead to interglacials, *Nature*, 542(7642), 427-432.
- Tzedakis, P., D. Raynaud, J. McManus, A. Berger, V. Brovkin, and T. Kiefer (2009), Interglacial diversity, *Nat. Geosci.*, 2(11), 751.
- Tzedakis, P., E. Wolff, L. Skinner, V. Brovkin, D. Hodell, J. F. McManus, and D. Raynaud (2012), Can we predict the duration of an interglacial?, *Clim. Past*, 8(5), 1473-1485.
- Venz, K. A., D. A. Hodell, C. Stanton, and D. A. Warnke (1999), A 1.0 Myr record of glacial North Atlantic intermediate water variability from ODP site 982 in the northeast Atlantic, *Paleoceanography*, 14(1), 42-52.
- Veres, D., L. Bazin, A. Landais, H. ToyÃ© Mahamadou Kele, B. Lemieux-Dudon, F. Parrenin, P. Martinerie, E. Blayo, T. Blunier, and E. Capron (2012), The Antarctic ice core chronology (AICC2012): an optimized

- multi-parameter and multi-site dating approach for the last 120 thousand years, *Climate of the Past Discussions*, 8(6), 6011-6049.
- Weber, S. L., S. S. Drijfhout, A. Abe-Ouchi, M. Crucifix, M. Eby, A. Ganopolski, S. Murakami, B. Otto-Bliesner, and W. R. Peltier (2007), The modern and glacial overturning circulation in the Atlantic Ocean in PMIP coupled model simulations, *Clim. Past*, 3(1), 51-64.
- Wunsch, C. (2006), Abrupt climate change: An alternative view, *Quat. Res.*, 65(2), 191-203.
- Yang, H. J., and J. Zhu (2011), Equilibrium thermal response timescale of global oceans, *Geophys. Res. Lett.*, 38, doi: 10.1029/2011gl048076.
- Zahn, R. (1994), Core correlations, *Nature*, 371(6495), 289-290.
- Zhang, R. (2008), Coherent surface-subsurface fingerprint of the Atlantic meridional overturning circulation, *Geophys. Res. Lett.*, 35(20).
- Zhang, X., G. Lohmann, G. Knorr, and C. Purcell (2014), Abrupt glacial climate shifts controlled by ice sheet changes, *Nature*, 512, 290-294.
- Zhang, X., G. Knorr, G. Lohmann, and S. Barker (2017), Abrupt North Atlantic circulation changes in response to gradual CO₂ forcing in a glacial climate state, *Nat. Geosci.*, 10, 518-523, doi: 10.1038/ngeo2974.

Figure 1 Location Map (a) Modern annual sea surface temperatures (SST [Locarnini *et al.*, 2010]) reflect the transport of heat into the Nordic Seas via the North Atlantic Current (i.e. the Nordic heat pump – see Section 3.3), which splits into the Irminger Current (IC) and Norwegian Current (NC). Hatched areas are approximate regions of modern deep water formation. Sites mentioned in the study (ODP 983, DSDP 609, MD01-2443 and NGRIP) are highlighted, as is the location of several deep ocean circulation reconstructions (green star) [McManus *et al.*, 2004; Roberts *et al.*, 2010; Henry *et al.*, 2016; Deaney *et al.*, 2017]. PF and AF are Polar and Arctic Fronts. (b) Modern (cope-top) distribution of *N. pachyderma* (%NPS) [Margo_Project_Members, 2009] reflects the SW-NE orientation of Polar and Arctic Fronts. (c) LGM distribution of %NPS [Margo_Project_Members, 2009] suggests southward shift of fronts and by implication a weakened Nordic heat pump. Maps were created with the ODV application [Schlitzer, 2014].

Figure 2 Changing atmospheric CO₂ and ocean conditions over the last 110kyr (see Fig. 1 for locations). From top to bottom: Records of IRD from DSDP site 609 [Bond and Lotti, 1995], sedimentary Pa/Th from the deep NW Atlantic (a proxy for AMOC strength) [McManus *et al.*, 2004; Böhm *et al.*, 2015; Henry *et al.*, 2016], atmospheric CO₂ [Bereiter *et al.*, 2015], dCO₂/dt (Methods Section 2.2), NGRIP $\delta^{18}\text{O}$ [NGRIP_members, 2004], NGRIP $\delta^{18}\text{O}_{\text{hi}}$ (Methods Section 2.2.1), SST from MD01-2443 [Martrat *et al.*, 2007], SST_{hi}. Numbered blue boxes represent cold (Heinrich) stadial periods. For lower 4 curves, dark pink areas represent the coldest quartile (25% of time) and light pink the warmest quartile. These relate to classes 1 and 4 respectively in Figure 3.

Figure 3 Changing CO₂ versus surface ocean conditions as shown in Fig. 2. (a) (Left) Rate of change of atmospheric CO₂ versus NGRIP $\delta^{18}\text{O}$ for discrete 200yr intervals. Coloured classes represent 25% of the population (i.e. a quarter of the time). (Right) Distribution of cumulative CO₂ rise (upper) and fall (lower) across NGRIP $\delta^{18}\text{O}$ classes as defined in (a, left) over the past 110kyr (horizontal lines at ± 0.25 indicate expected value if there were no systematic relationship). (b) Same as (a) but for NGRIP $\delta^{18}\text{O}_{\text{hi}}$. (c, d) Same as (a, b) but for MD01-2443 SST and SST_{hi}. See Methods Section 2.2 for explanation.

Figure 4 Rate of change of atmospheric CO₂ versus GL_{T_syn_hi} for discrete 200yr intervals

over the past 800kyr. Coloured classes represent 25% of the population (i.e. a quarter of the time). (Right) Distribution of cumulative CO₂ rise (upper) and fall (lower) across GL_{T_syn_hi} classes over the past 800kyr. High absolute values of GL_{T_syn_hi} (e.g. classes 1 and 4) represent intervals when the AMOC is furthest from equilibrium i.e. anomalously weak (negative GL_{T_syn_hi}, class 1) or strong (class 4) (see Methods Section 2.3). Note similarity with right hand panels of Fig. 3b, d, which represent only the last 110kyr.

Figure 5. 800kyr of abrupt climate variability. (a) Integrated northern summer insolation (black curve) [Tzedakis *et al.*, 2017]. (b) Benthic foraminiferal $\delta^{18}\text{O}$ stack (blue) [Lisiecki and Raymo, 2005]. (c) GL_{T_syn}, a prediction of northern abrupt climate variability (green) [Barker *et al.*, 2011]. (d, e) IRD/g (blue filled) and %NPS (pink filled) from ODP site 983. (f, g) atmospheric CO₂ and dCO₂/dt (purple). (h) %NPS_{hi} (red; Methods 2.2.1). (i) Wavelet transform of %NPS, produced using the Matlab function given by Grinsted *et al.* [2004] and implemented on the %NPS record after evenly resampling at 100yr intervals (white curve is the LR04 benthic stack). T1-9 are glacial terminations; #1-19 are MIS; coloured boxes as in Fig. 7 annotation. Red and green circles in (a) are peaks in summer energy that (respectively) do and do not cross the threshold for producing an interglacial state [Tzedakis *et al.*, 2017]. T6 and T8 represent protracted terminations (see text).

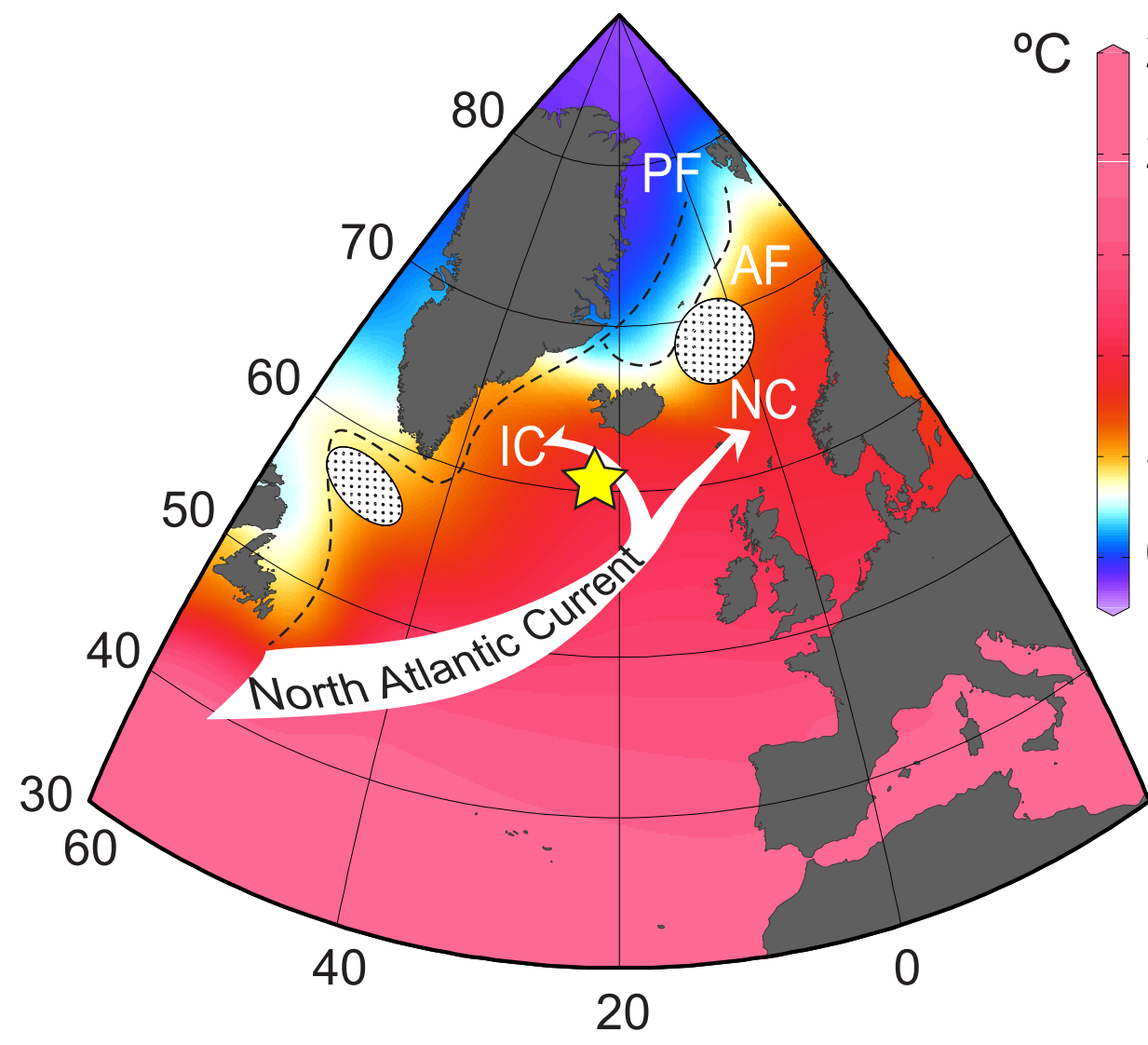
Figure 6 Changing CO₂ versus surface conditions across the North Atlantic region over the past 800kyr. (a) %NPS_{hi} versus IRD/g from ODP 983, colour-coded by contemporaneous rate of CO₂ change (left) or mean dCO₂/dt for each sector (right). Each dot represents a discrete 200yr interval. Sector X (Y) represents the coldest (warmest) AND iciest (least icy) intervals. (b) Box plots showing the distribution of dCO₂/dt for each sector in (a). (c) (Left) Distribution of cumulative CO₂ rise (upper) and fall (lower) across IRD/g classes as defined in (a) over the past 800kyr. (Right) same as left but using IRD accumulation rate instead of IRD/g. (d) (Left) Distribution of cumulative CO₂ rise (upper) and fall (lower) across %NPS_{hi} classes as defined in (a) over the past 800kyr. (Right) same as left but with %NPS_{hi} shifted by -1000yr (see text). For all parts class 1 represents the coldest (or iciest) quartile (25% of the time) and class 4 the warmest (or least icy).

Figure 7 Glacial terminations of the last 800kyr. All panels from top to bottom: Integrated summer insolation [Tzedakis *et al.*, 2017] (coloured circles as in Fig. 5), Antarctic temperature proxy (δD) [Jouzel *et al.*, 2007], atmospheric CO₂ [Bereiter *et al.*, 2015], atmospheric CH₄ [Loulergue *et al.*, 2008], IRD/g, %NPS, benthic foraminiferal $\delta^{13}\text{C}$ [Channell *et al.*, 1997; Raymo *et al.*, 2004] and %NPS_{hi} all from ODP 983, GL_{T_syn_hi} [Barker *et al.*, 2011], benthic $\delta^{18}\text{O}$ from ODP 983 [Channell *et al.*, 1997; Raymo *et al.*, 2004] (green) and the LR04 $\delta^{18}\text{O}$ stack on its independent age model [Lisiecki and Raymo, 2005] (black). Blue boxes represent main deglacial phase of ice rafting until start of interglacial conditions according to definition 1 (see text). Pink boxes represent intervals of anomalous surface warmth (low %NPS_{hi}) and strong AMOC (high GL_{T_syn_hi}) prior to the start of equilibrium interglacial conditions according to definition 2 (see text). Records from nearby core RAPID-17-5P [Thornalley *et al.*, 2010] are used instead of those from ODP 983 over the interval 7.5-21.3ka due to the lower quality benthic $\delta^{13}\text{C}$ record from 983 across this interval.

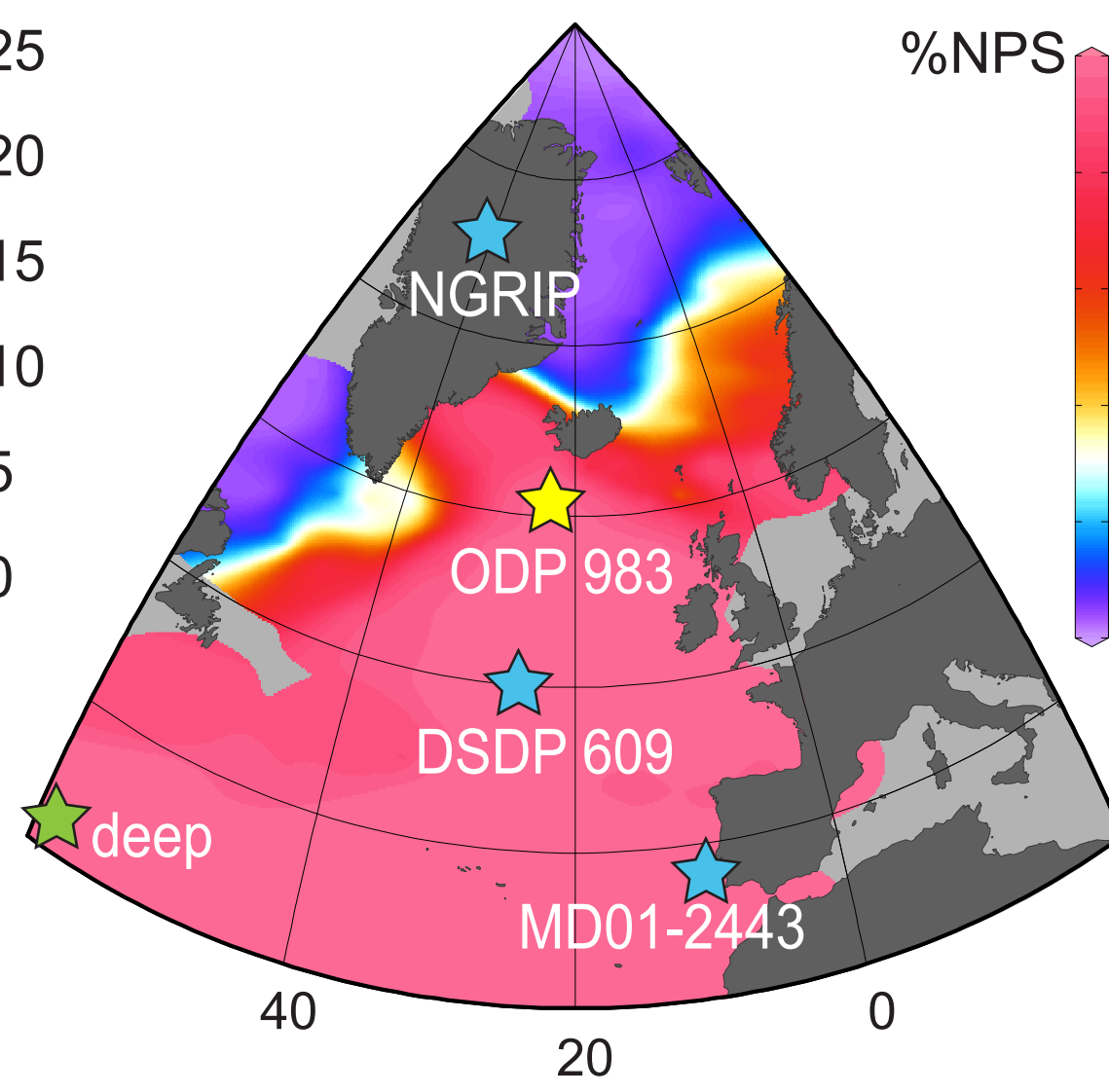
Figure 8 Individual deglacial transitions according to definitions 1 (left hand panels) and 2 (right hand panels) for the start of interglacial conditions. **(a, b)** Benthic $\delta^{18}\text{O}$ [Lisiecki and Raymo, 2005] versus atmospheric CO_2 [Bereiter *et al.*, 2015] (arrow is schematic representation of deglacial trend, see also Fig. S6). **(c, d)** $d\text{CO}_2/dt$ versus %NPS from ODP 983. **(e, f)** $d\text{CO}_2/dt$ versus IRD/g. **(g, h)** %NPS_hi versus IRD/g (partitions and labels as in Fig. 6). T1-9 are terminations 1 to 9 with colour coding the same in each panel.

Figure 1.

(a) Modern SST



(b) Modern %NPS



(c) LGM %NPS

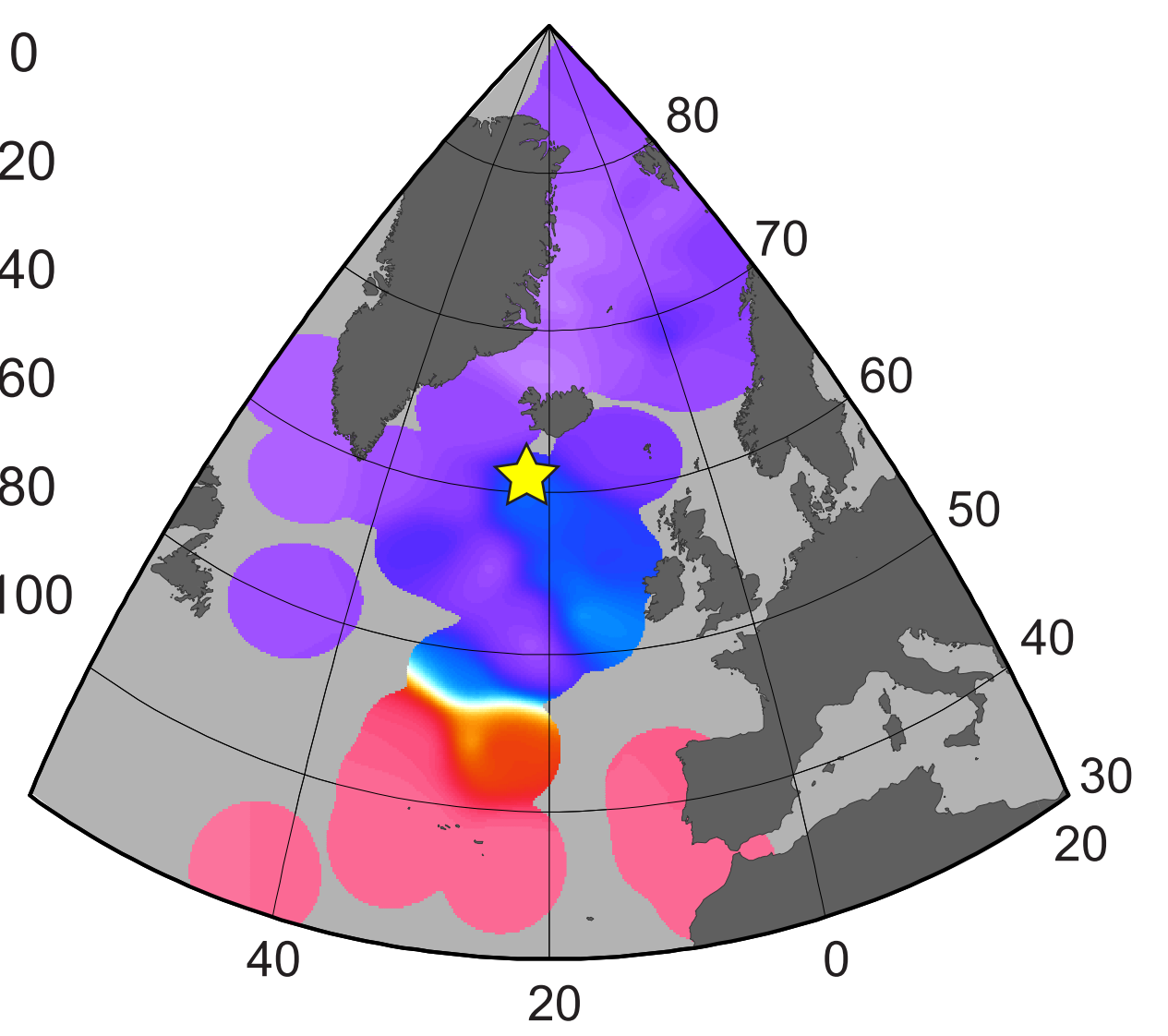


Figure 2.

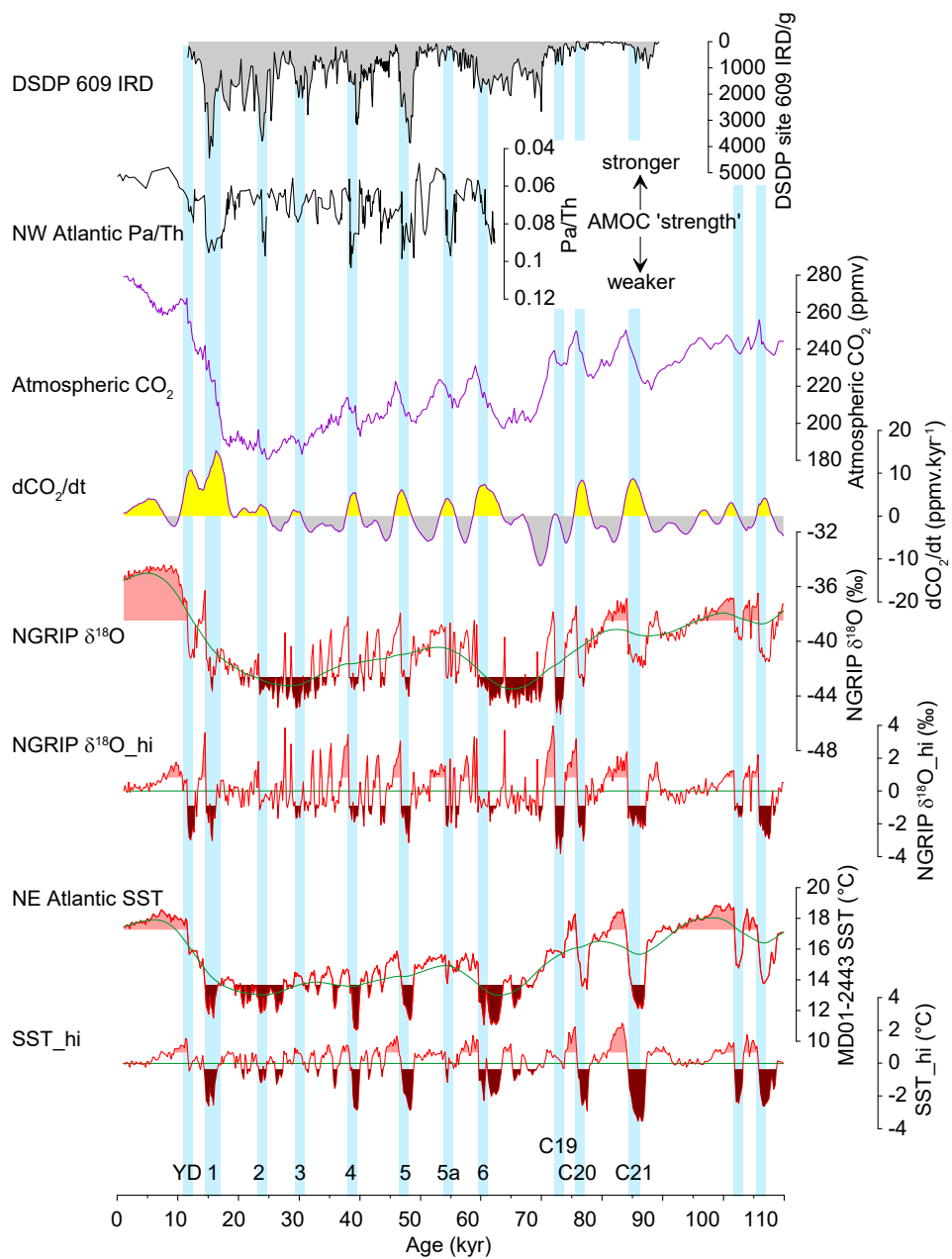
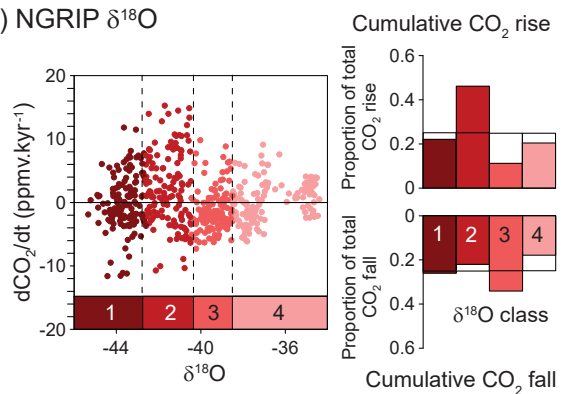
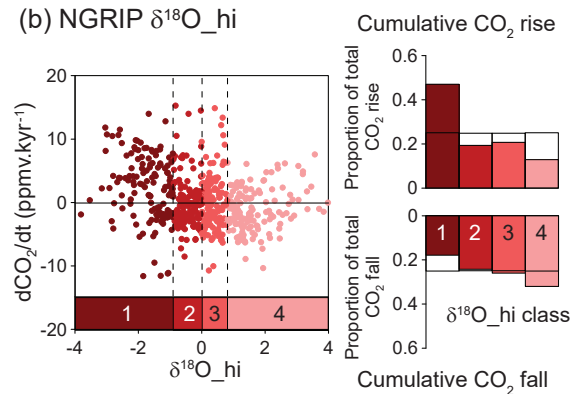


Figure 3.

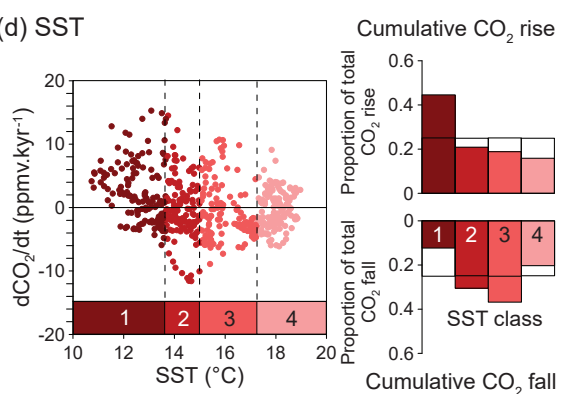
(a) NGRIP $\delta^{18}\text{O}$



(b) NGRIP $\delta^{18}\text{O}_{\text{hi}}$



(d) SST



(e) SST_{hi}

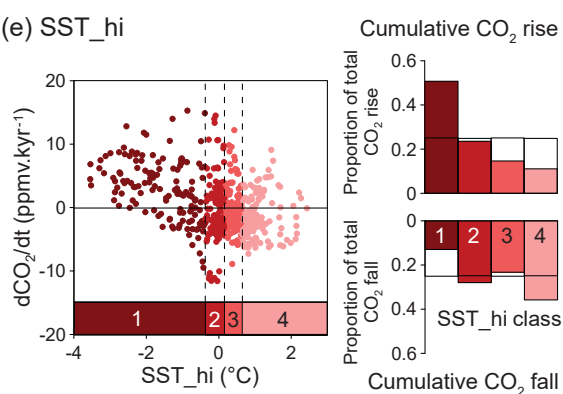


Figure 4.

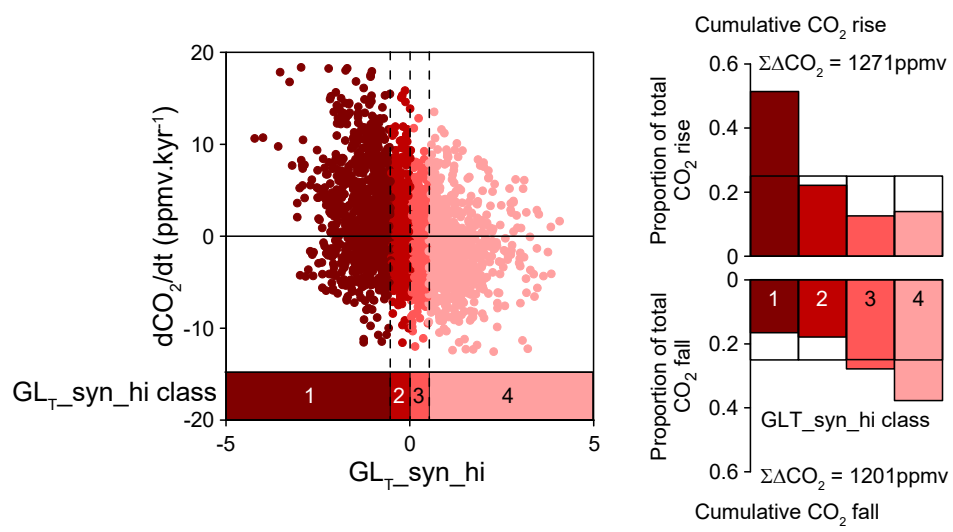


Figure 5.

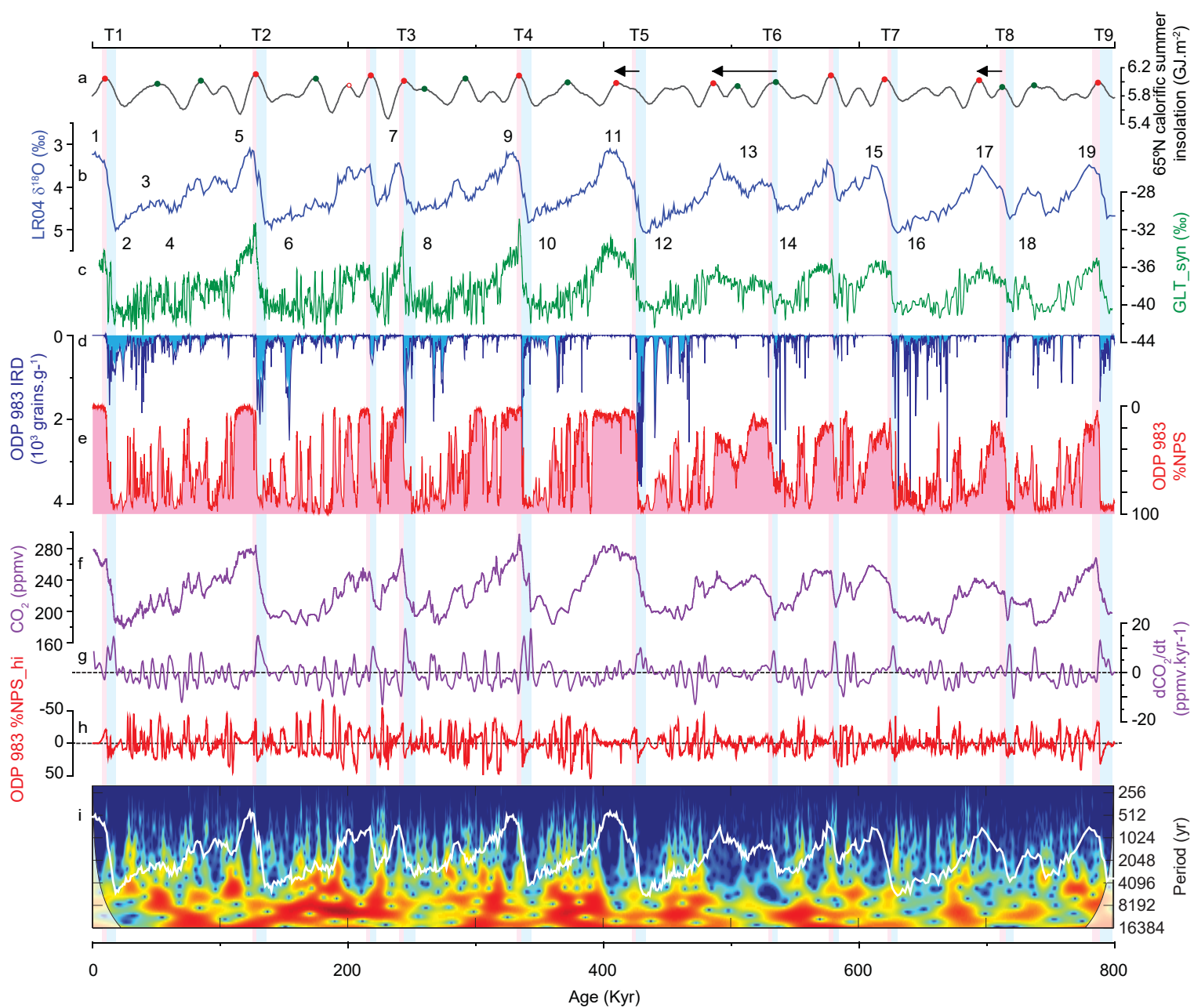


Figure 6.

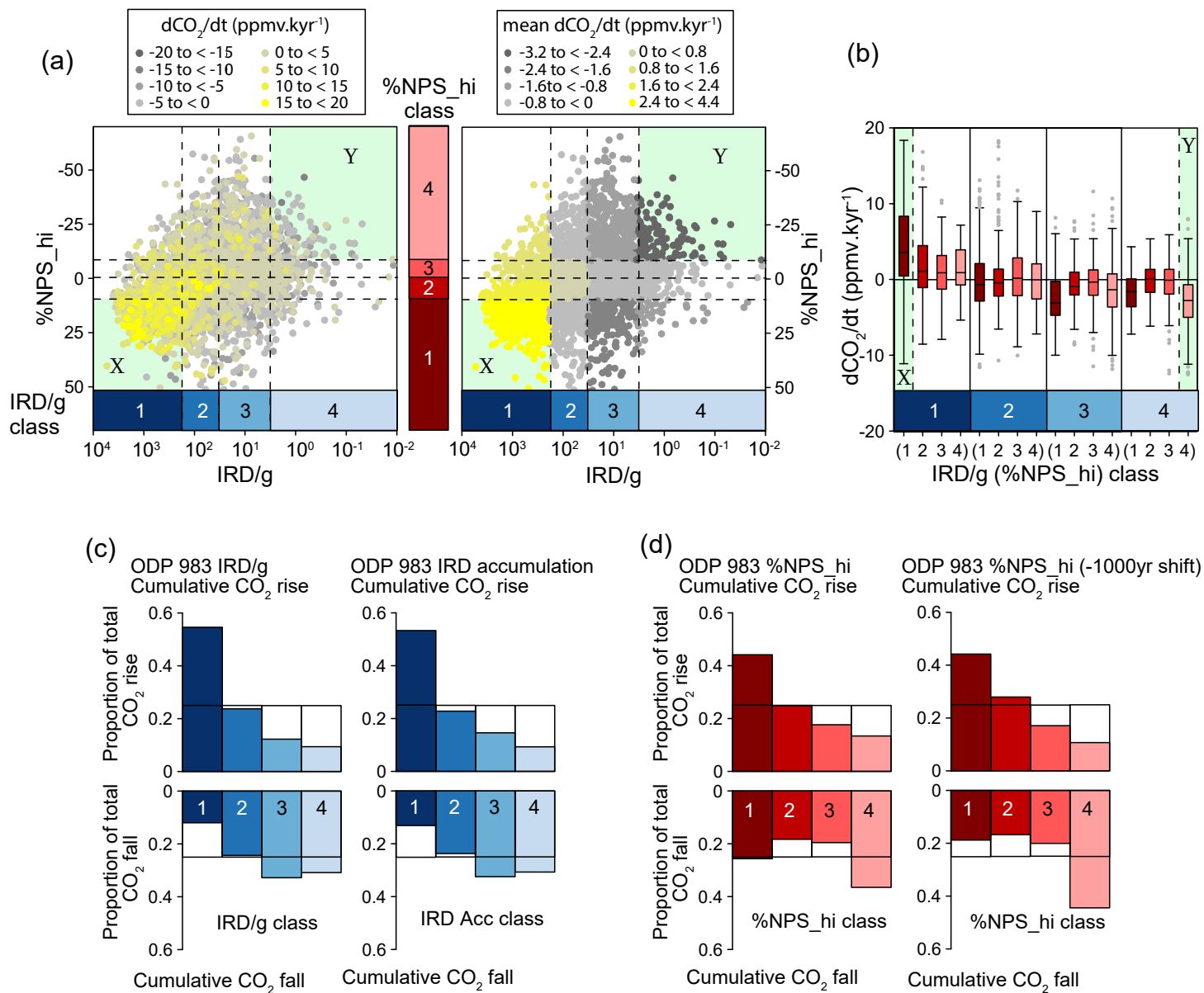


Figure 7.

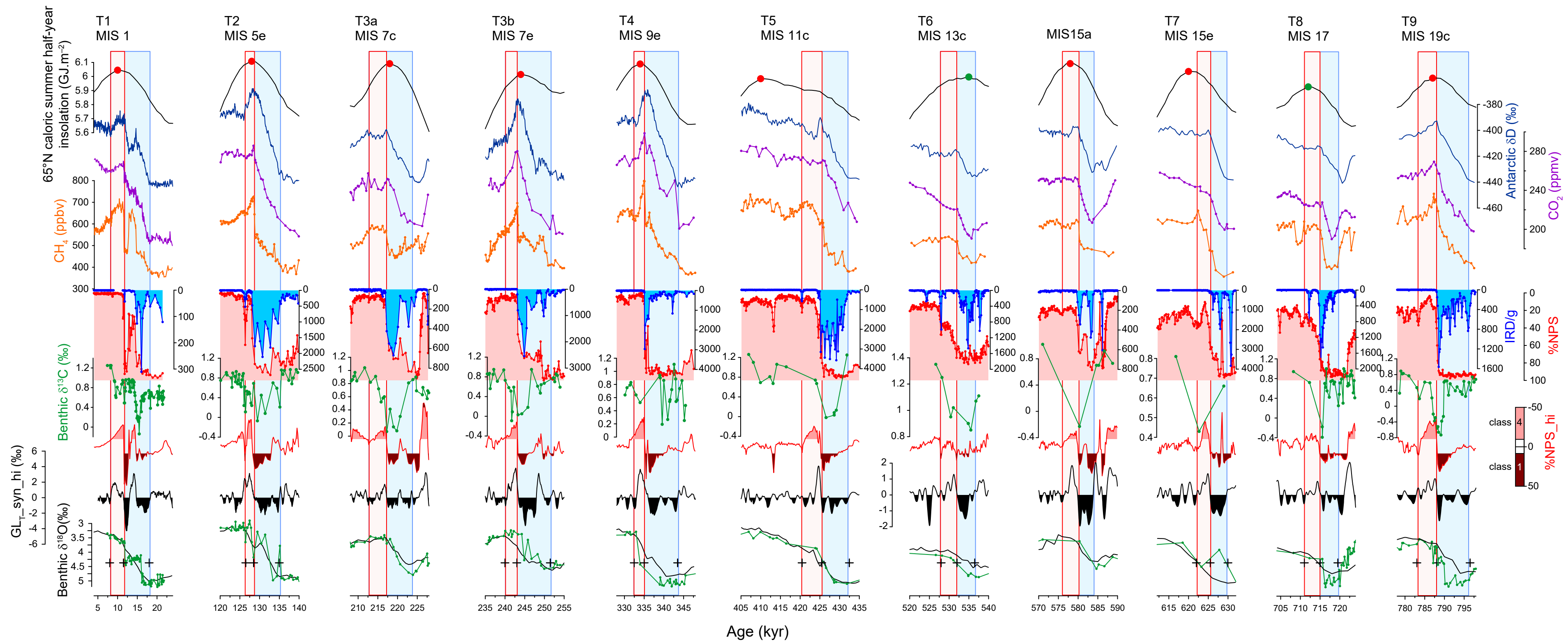


Figure 8.

